Addis Ababa Institute of Technology
School of Graduate Studies
School of Mechanical and Industrial Engineering

Thermal Engineering Stream

Design and CFD Analysis of a Micro Kaplan Turbine Runner

By: Getachew Tikue

A Thesis Submitted to The School of Graduate Studies of Addis Ababa University In Partial Fulfillment of The Requirements of The Degree of Masters of Science In Thermal Engineering.

Advisor

Dr.-Ing. Edessa Dribsa

Co-Advisor

Tilahun Nigussie

Addis Ababa, Ethiopia

June 6, 2018

Addis Ababa Institute of Technology

Graduate Studies

School of Mechanical and Industrial Engineering

Thermal Engineering Stream

Design and CFD Analysis of a Micro Kaplan Turbine Runner

By: Getachew Tikue

Approved by the Examining Board:

Dr.Kamil Dino	_____	_____
Chairman, Department of Graduate Committee	Signature	Date
Dr. Ing. Edessa Dribsa	_____	_____
Advisor	Signature	Date
Ato Tilahun Nigussie	_____	_____
Co-Advisor	Signature	Date
Dr. Yilma Tadesse	_____	_____
Internal examiner	Signature	Date
Dr.–Ing.Wondowesen Bogale	_____	_____
External Examiner	Signature	Date

SIGNED DECLARATION

I declare that the thesis for the M.Sc. degree at the University of Addis Ababa, here by submitted by me, is my original work and has not previously been submitted for a degree at this or any other university, and that all reference materials contained therein have been duly acknowledged.

Name: Getachew Tikue

Signature: _____

ABSTRACT

Utilization of Micro hydro power as renewable energy source is giving great attention now a days. This micro hydropower energy can be obtained from potential hydro sites with sufficient water discharge and pressure head. Depending upon the sites, water turbines are designed and manufactured to avail hydropower energy. Low head turbines are widely used on run of rivers and they classified under reaction turbines. They operate at higher flow rate, smaller head and faster rotational speed, thus being more compact than other types of machines.

With the increasing cost of energy and the high demand of green energy, the micro hydro Kaplan power plants gain special attention. The development of micro hydro Kaplan power plants on large scale will generate enough energy for the rural community and are being economically profitable. They comprise runner and draft tube and the efficiency of hydro Kaplan reaction turbine is significantly affected by the performance runner.

In this present work focused on the design and CFD analysis of a micro Kaplan runner for selected potential site called Denkaka village which is located in Oromia Region, Ethiopia. This runner design and performance improvement is prime concern. In this research, size of the runner was determined using formulas depend on the site data of 3.125m gross head and 0.6m^3/s fluid flow rate. Geometrical parameters (D_{tip} =0.4m, D_{hub}=0.15m, n_{max}=26s^{-1} and net power capacity is 14.7 kW) are to be determined.

Different tools were used to run simulations. These include XFLR5 soft-ware to determine NACA2412 coordinate pointes of blade profile, Solid work used to make solid 3D model of the runner and ANYS CFX to do its volumetric meshing, fluid flow simulation, for numerical flow analysis and to evaluate the hydraulic performance of the runner. The complete flow pattern is numerically simulated using k-ε model. Simulations have been carried out by varying fluid flow rate and runner speed of the turbine.

Research results show 14.7kW of net hydraulic power output and 91.6% hydraulic efficiency were generated. Also as obtained from the pressure contour analysis, there is maximum at the leading edge and then decreases towards the trailing edge. The results obtained from flow simulations were found to be in accordance with turbine characteristics curves. The comparison shows that there is close similarities between present and Dr. Ruchi Khare work.

Keywords: Micro Kaplan, Runner Blade, CFD, Hydropower, Renewable energy.

ACKNOWLEDGMENT

I would like to thank the school of mechanical and industrial engineering of the Addis Ababa Institute of Technology, Addis Ababa University.

I would like to express my special appreciation to my advisor, Dr.-Ing. Edessa Dribsa for his expert guidance, constructive comments, support and kindness in helping me in the completion of my thesis. His academic support was instrumental throughout the research project. I would like also to recognize my co-Advisor Mr.Tilahun Nigussie for his everlasting support throughout this thesis work.

TABLE OF CONTENTS

LIST OF TABLES

LIST OF FIGURES

LIST OF NOMENCLATURES

P	Power
ρ	Density of water
G	Gravitational acceleration
Q	Discharge
U	Average tangential velocity
W	Relative velocity
V_w	Tangential absolute fluid velocity of water
A	Cross sectional area of river
C	Absolute velocity
D_{tip}	Runner diameter
D_{hub}	Hub diameter
t_s	Space between each blade
E	Specific hydraulic energy of machine
ΔB	Width between two successive depth and velocity measuring points
H	Gross head
Hh	Hydraulic efficiency
H_n	Net head
H_s	Suction head
L	Chord length
P_{min}	Minimal water pressure
r	Mean radius

n_{max}	Runaway speed
ω	Angular velocity
n_{QE}	Specific speed
V_{mean}	Mean velocity of the flow
β	Blade Angle
α	Angle of attack
Λ	Angle of slip
C_L	The lifting coefficients for each radius
C_D	Drag coefficient
Re	Reynolds number
N	Runner rotational speed
P_{atm}	Atmospheric pressure
P_v	Vapor pressure

LIST OF ABBREVIATIONS

MHP	Micro Hydro Power
NACA	National Advisory Committee for Aeronautics
RANS	Reynolds Average Navier Stoke
CFD	Computational Fluid Dynamics
CAD	Computer Aided Design
KW	Kilo Watt
MWIE	Ministry of Water, Irrigation and Energy
CMM	Coordinate Measuring Machine
BIA	Blade Inclination Angle
GVO	Guide Vane Opening
RSIF	Rotating stationery interface
IMF	International Monetary Fund

CHAPTER ONE

INTRODUCTION

This chapter is an introduction to the work performed during this research and describes the purpose of it. An overview of research background, significance of the study followed by objectives of the research, research methodology and scope of the study are provided here. Organization of the thesis and a brief description of the following chapters are provided at the end of this chapter.

1.1 Background and Significance of Study

Demand for increasing the use of renewable energy has risen over the last two decades due to environmental issues [1]. To help rural people to improve their financial condition and get better life-style, application of small-scale hydro or micro-hydro power has proved as a very successful tool [2].Therefore, it has been increasingly used as an alternative energy source, especially in remote areas where other power sources are not viable.

The Ethiopian Highlands are Africa's largest continuous mountain range. Ethiopia is often referred to as the "water tower" of Africa because of its abundant water resources, the greatest in the whole of Africa. According to the International Monetary Fund (IMF), at one time Ethiopia had one of the fastest growing economies in the world, but despite this it contends with poorness. The economy faces a number of serious problems, which are addressed with a focused investment in public infrastructure and industrial parks. The economy's progress is highly dependent on the development of the nations' hydro resources. Only 25% of the population has access to electricity today and the government plans to increase this up to 75% within the next five years.

Ethiopia has the second largest hydropower potential in Africa, with only 10% developed to date but nonetheless covering 90% of the nation's electricity demand. Currently, installed capacity is about 4,330 MW of hydro, but more than 6,600 MW are under construction. By 2020, about 14,000 MW could be in operation. Denkaka is one of the remote areas which could not get access of electricity but has a nearby micro hydro resource site. It is in Adda Woreda found in

oromia Zone located 50 km from Addis Ababa in North West direction geographically situated at East-South 34° from Mojo on the coordinate of 8.67°N, 39.03°E. The micro hydro potential near by the village has the capacity to generate about 14.7kW of electricity during the dry season [Source: measuring during dry season, March]. Moreover, the need for development of micro hydro turbines using locally available materials and with local manufacturing capability has been identified. The aim being to cut the equipment cost which is imported from various countries in Europe and Asia [3].

Micro Hydro-Turbines (MHTs) refer to turbines with capacity ranging from 5kW which is just enough to provide domestic lighting to a group of houses through a battery charging to 100 kW which can be used for small factories and to supply an independent local micro-grid [3].Most of these turbines are not different from small or large hydro turbines. For example the principles of operation, types of material units, and the mathematical equations used in the selection and design of turbines are mostly the same as large hydro turbines.

Basically, hydraulic turbines are classified into two, namely, impulse type and reaction. The impulse turbine like Pelton, Turgo and cross flow type convert the potential energy of water in to kinetic energy in a jet issuing from a nozzle and projected onto the runner buckets or vanes. The reaction turbine like Kaplan, Propeller, and Francis turbines develop power from the combined action of pressure energy and kinetic energy of the water. Rotary action of the water turbine in turn drives an electrical generator that produces electrical energy or could drive other rotating machinery. It is very important to predict the hydraulic behavior and efficiency of hydro turbines before they are put in actual use. The experimental approach for determining the performance of hydro-turbines is costly and time consuming. Moreover, the result so obtained can rarely give indications for the causes of poor performances. Computational Fluid Dynamics (CFD) on the other hand has become today‘s state-of-the-art technique in hydro-turbines. Therefore, the design of turbines needs to be developed by means of CFD simulations in order to optimize and enhance efficiency. With these technologically advanced tools, important flow features could be predicted with high accuracy. This allows the performance, efficiency and cavitation limits of a turbine to be predicted realistically for different operating conditions before fabrication process [4]. Most of the past studies have focused on the draft tube for increasing the efficiency of the plant, but a

good draft tube design is not enough. Recent studies have shown that the efficiency improvement can also be realized by minor modification on the older design in there runner blades and spiral casing. Previous studies have shown that there is potential for increasing unit performance by a moderate modification of such runner blades. Runner blades have been found to have an efficiency loss due to the runner losses. A small increase in performance in these power stations represents a considerable economic value.

As a result, the aim of this thesis work is to design, model and perform CFD analysis of a micro Kaplan turbine runner to provide a great contribution on the implementation of hydro power plant on the site selected. The designed 3D model of turbine runner flow simulation is carried out using ANSYS-CFX 15.0 package. The variation of flow parameters from hub to tip of runner are presented in graphical form and average value of cascade parameters are computed at different operating regimes. The results obtained from CFD are of great interest since these findings can be used to minimize testing time and cost as well as to analyze failure conditions. Through the process, the research aims at building the local capacity needed for affordable and sustainable development of the resources for the benefit of those citizens dwelling nearby the selected site.

The significances of this research project are:

i. The technology will be beneficial to local runner manufacturing industries and will thus ensure availability of the turbines runner locally at low cost.

ii. It provides information to various stakeholders and contributes knowledge to micro hydro power research.

iii. The results of the research will ensure availability of documented procedures for designing of micro hydro turbine runner in Ethiopia.

1.1.1 Over View of Kaplan Turbine Technology

Kaplan turbine is an axial flow reaction turbine. This operates in an entirely closed conduit to tailrace. It is employed, where a large quantity of water is available. It consists of spiral casing, guide mechanism. The runner in a Kaplan turbine is a very challenging part to design [1]. The propeller shaped runner is mounted vertically with several blades. The Kaplan turbine has

adjustable blades and was developed on the basic platform (design principles) of the Francis turbine by the Viktor Kaplan in 1913. The main advantage of Kaplan turbines is its ability to work in low head sites which was not possible with Francis turbines. Kaplan turbines are widely used in high-flow, low-head power production. The Kaplan turbine is an inward flow reaction turbine, which means that the working fluid changes pressure as it moves through the turbine and gives up its energy. The design combines radial and axial features. The inlet is a scroll-shaped tube that wraps around the turbine's wicket gate. Water is directed tangentially through the wicket gate and spirals onto a propeller shaped runner, causing it to spin. The outlet is a specially shaped draft tube that helps decelerate the water and recover kinetic energy. The turbine does not need to be at the lowest point of water flow, as long as the draft tube remains full of water. A higher turbine location, however, increases the suction that is imparted on the turbine blades by the draft tube that may lead to cavitations due to the pressure drop. Typically the efficiencies achieved for Kaplan turbine are over 90%, mainly due to the variable geometry of wicket gate and turbine blades. This efficiency however maybe lower for very low head applications. Since the propeller blades are rotated by high-pressure hydraulic oil, a critical design element of Kaplan turbine is to maintain a positive seal to prevent leakage of oil into the waterway. Kaplan turbines are widely used throughout the world for electrical power production. They are especially suited for the low head hydro and high flow conditions – mostly in canal based hydro power sites [1].

The experimental testing of turbine models at different operating regimes on specially designed test rigs is the conventional approach to assess the performance but its expensive and time-consuming tests. The flow in axial flow turbine (Kaplan) is very complex including several flow phenomena, such as turbulence, separation, swirling flow and unsteadiness flow. Advanced fluid flows are described by the continuity and momentum equations, which can generally not be solved analytically.

Therefore, the numerical procedure in computational fluid dynamics (CFD) is of highest importance. CFD can be used to check efficiency of alternate designs [5,6] of turbines for optimization before final experimental testing of selected designs in resorted. However, in order to prove reliability of these tools for application to turbines, validation or verification [4,7] is

required. This research was carried out in order to design, model and perform CFD analysis of a micro Kaplan turbine runner for the selected site in Ethiopia called Denkaka.

1.2 Objectives of the Thesis

1.2.1 General Objective

The overall objective of this thesis is to design, model and perform CFD analysis of a micro Kaplan turbine runner and making performance characteristic curves of the turbine runner which could ultimately be used for electrification of Denkaka village in Adda district which is in the vicinity of Modjo River.

1.2.2 Specific Objectives

To achieve the proposed goal, the research has the following specific objectives:

1. Determination of the micro hydro power potential of the site from the available head and flow rate data of the water resource nearby the Denkaka village.
2. Select a suitable turbine runner using turbine selection chart.
3. Determine geometrical dimensions of the turbine runner based on those design data;
4. Make 3D modeling and perform performance simulation of the turbine runner using CFD.
5. Analyze CFD result and interpret the results.
6. Verify results obtained using that of V.Chandrakar, R.Khare research work [8].
7. Accept final result and write conclusion.

1.3 Scope of the Study

The scope of the study is to design, model and perform CFD analysis of a micro Kaplan turbine runner to predict performance of the blades of a micro-Kaplan turbine hydro power used for station with the help of CFD tool. The study will provide a great contribution on the application of renewable energy to satisfy the energy demand of the village selected.

This study shall collect and analyze relevant data of the site and select the most suitable turbine type, recommend necessary actions that can configure an optimum model design to have contribution on accommodation of the current and near future electrical energy demand for the village. The study only focuses on design and CFD analysis of a micro Kaplan turbine runner

among different components, like guide vane, spiral casing. Experimental test is not performed in this study.

1.4 Outline of the Thesis

This section provides an outline of the thesis and briefly describes the contents of the following chapters.

Chapter one: is an introduction to the work performed during this research and describes the purpose of it. An overview of research background, significance of the study followed by objectives of the research, research methodology and scope of the study are provided here. Organization of the thesis and a brief description of the following chapters are provided at the end of this chapter.

Chapter two: is a literature review part in which different literatures related to the design of Kaplan turbine runner and conical type draft tube are reviewed. Some of the related works studied by different researchers including their detail suggestion and conclusion are reviewed. Short comings of some of the methodologies applied in the literatures compared to the present work are reviewed. Summary of the chapter is also presented at the end of this chapter.

Chapter three: describes the design process of a Micro Kaplan turbine runner. Determining of runner size, process of geometry parameterization, calculation of main-dimensions and development of Kaplan turbine runner using the related empirical formulas are briefly overviewed in this chapter.

Chapters four: provides a brief and detail description to the CFD analysis of 3D model of Kaplan turbine runner to perform further performance evaluation for the designed Kaplan turbine runner. A complete workflow for one CFD simulation of the designed 3D model of Kaplan turbine runner followed to objective and challenges to CFD analysis of the runner is described in this chapter.

Chapter five: provides a discussion on the CFD results obtained. This includes assessment of the hydraulic efficiency, power output and total torque obtained from CFD simulation of turbine runner. Graphs of characteristic curve of the runner are presented in this chapter. Verification

between the present work and Dr. Ruchi Khare [8] research work are also provided in this chapter.

Chapter six: is the final chapter that summaries the outcomes of the research and reflects on the goals set and success in meeting them. Recommendations for the future work are also provided in this chapter.

CHAPTER TWO

LITERATURE REVIEW

This chapter is a literature review part in which different literatures related to the design of Kaplan turbine runner are briefly discussed. Some of the related works studied by different researchers including their detail suggestion or conclusion are reviewed. Short comings of some of the methodologies used by the previous researchers compared to the present work are reviewed at the end of this chapter.

2.1 Related Works

Several researches have been conducted on design and development of small scale Micro hydro turbine runner in many developing countries. Different methods and approaches have been used to develop and improve the performance of hydro turbine. Optimizing of runner blade is one of them used to improve turbine efficiency. Therefore, a numbers of research results studied by a number of researchers have been published. Some of the research papers are reviewed in the following paragraphs.

Timo Flaspohler [9]. Conducted a research for his doctorial dissertation entitled the “Design of the runner of Kaplan turbine". His study aimed at designing a Kaplan turbine runner which was used in small hydroelectricity power plant in Finland. Different methods, steps and assumptions were applied in determination of the runner size. He started the process by identifying the main characteristics of the runner he wanted to design and had a sketch of the turbine runner with parameters labeled. (And then detail procedures used with brief descriptions, including formulas, were discussed). The input power supplied by the runner has to be calculated first using density of the fluid, acceleration due to gravity, head net and maximum discharge. To determine the speed of the turbine; in doing that he calculated the specific speed which is a dimensionless parameter and characterizes the hydraulic properties of a turbine in terms of speed and discharge capacity; the rotational speed from which the synchronous speeds will be derived and will be used to determine the speed which the runner should reach to connect it directly to the generator. The runaway speed is the maximum speed in which the turbine runner can rotate freely without a load. The runner and hub diameter section has to be determined from empirical formulas using

the available head and flow rate. After he fixed the diameter, the blade characteristics under different head and discharge for different circumstance was tabulated. The suction head and cavitation coefficient was to be calculated so that cavitation would not occur. Finally, the blade designed by considering factors playing significant role other than stress analysis. Authors observed that leading edge was thicker than the trailing edge for a streamlined flow. Furthermore, the blade designed to be as thin as possible to improve the cavitation effect; it was thicker near the hub becoming thinner and thinner towards the tip. In addition, the blade had been distorted on the basis of the tangential velocity. The Tragflügel theory played an important role in defining the shape of the profile by applying different assumptions, charts and empirical formulas and his analysis was carried out using standard equations. After all he was able to get the dimensions of the runner and determine the geometry and size of the turbine runner.

L.Motycak and J.Obrovsky [10]. Studied research work entitled on "Analysis of the Kaplan turbine draft tube effect". The study was aimed to present information about possible problems and errors which can appear during numerical analyses of low head Kaplan turbines with a view to the runner - draft tube interaction. They used the setting of numerical model, grid size and used boundary conditions are the interface definition between runner and draft tube. Available data from physical model tests which give a great opportunity to compare CFD and experiment results and was used to determine the approach to the CFD flow modeling. The Kaplan turbine model measurement was used to gather the information about real flow field. They perform model tests and were focused on the detailed velocity measurements downstream of the runner. The data's from CFD simulation were compared to the velocity measurement results. At the end results were confirmed by model tests in the hydraulic laboratory as well.

Y. Myint and H. Win [11]. Conducted research work entitled on "Design and Flow Simulation of Runner Blade for Kaplan/Propeller Turbine". The main purpose of the study was to develop the living standard in rural areas and to reduce the use of non- renewable energy. They started their work by the design of the turbine runner blade according to the specific conditions of water potential of the site of operation using different procedures. Flow simulation was utilized for predicting the flow analysis of runner blade. The 2D and 3D model of turbine runner blade was drawn by using Solid Works software. They can be used at sites having a value of head 1.5m and

flow rate 1.499m3/s. Lastly they suggested that design of the runner blade is a quite complex part; so it caused a lot of difficulties to draw in a proper way however, it is the main factor for optimizing the Kaplan turbine runner.

Ruchi Khare (Dr.) and V. Prasad (Dr.)[12]. Studied research work entitled "Design optimization of conical draft tube of hydraulic turbine". The study showed the flow and head recovery of draft tube. In the study the performance of draft tube was analyzed by calculating head loss, head recovery coefficients and efficiency of draft tube from simulation results. The head recovery is more influenced at smaller length but has very negligible change after the length equal to 19D. The rate of change in recovery due to cone angle is more at small length of draft tube. The efficiency variations indicated that efficiency had gradually increased as the L/D ratio increased up to 19 but after that effective increase of efficiency was very less due to small increase in recovery so increasing the length beyond 19D would not prove economical and also lead to problem of cavitation in turbine. The most of the hydro power plants have used straight conical draft tube, diffuser angle 3.6^0 to 6^0 and hence the results from numerical simulation were validated and were accepted.

Diaelhag Khalifa[13]. Conducted research work entitled on "Simulation of an axial flow turbine runner's blades using CFD". The aim of the study was to use computational fluid dynamics software package (CFX) to study and analyze flow's behavior in an axial flow turbine. He used blades of Kaplan turbine runner to produce a power. The study was focused on the variations of velocity components and the pressure by average circumferential area from inlet to outlet of the blades and used as factors to analyze the flow inside the blades. The research study indicated that, performance of the designed blades is acceptable and results of the analysis has shown a good prediction of the flow behavior inside the blades and was lead to acceptable blade design, which can be used in Kaplan turbine.

Williams, A. et.al [14]. Worked research project entitled "Developing standard design procedure for Pico propeller/Kaplan turbines". The study aimed to develop standard design procedure of Kaplan turbine for local manufacturing in the developing countries. A5kW demonstration turbine was set up at a test site in Peru. CFD has been used to obtain overall performance data for the turbine and to assist in the design of a new runner. It was found that due to the improper

adjustment of runner design and operating speed an incorrect matching between the runner design and the available flow rate at the site significantly affected the turbine operation. He suggested that in order to provide an acceptable performance it was possible to adjust the runner design and operating speed of the turbine. Authors concluded that the computational fluid modeling can be used as an appropriate design tool.

Yohannis Mitiku et.al [15]. Conducted a research work entitled "Modeling, Simulation and Optimization of Very low head axial flow turbine runner." The study aimed to achieve an efficient turbine runner and to produce a power of 1kW at a head less than 1m from flowing river. FLUENT software was used to define the geometry and solve flow to analysis fluid flow through the blade. Flow rate, rotational speed, blade inclination angle and number of blades are parameters used by the authors in CFD modeling and simulation of the runner. The computed result show that power developed by turbine runner increases with increasing flow rate. Pressure inside the runner increases with flow rate but, runner efficiency increases for some flow rate and almost constant thereafter. Efficiency and power developed by a runner drops quickly if turbine speed increases due to higher pressure loss and conversion of pressure energy to kinetic energy inside the runner.

A study was conducted by **Nabil H. Mostafa and Mohamed Adel [16].** Entitled on "Unsteady Numerical Simulation of axial turbine". They carried out 3D numerical study in order to study the unsteady flow, turbulent and cavitation simulation inside the passage of the axial flow turbine. In their study, a 3D Navier-Stokes code was used to model the flow field around a four blades axial turbine. The governing equations were discretized on a structured grid using an upwind difference scheme. The standard k-ε turbulence model was used for numerical simulation to account for the turbulence effect. Pressure distribution was completed versus time at different condition. The computational code has been validated by comparing the predicated numerical results with the previous studies. Finally the comparison has shown a good agreement.

Generally, research review on the previous work shown above indicates that attempt on the research work on subject area is rare. In the reviewed research work as referred in this section [9-16], it is to be pointed that most of the optimization work has been carried on the runner blade by changing blade shape. On the other hand, research review on the previous work observed that no

researcher use any kind of software to get the coordinate pointes of NACA profile, almost all of them were used either coordinate measuring machine (CMM) or Google internet. But using this method has certain short comings compare to present work. This is because of time consuming, coasty and very limited to get the coordinate points of NACA airfoil.

Researchers studied in the previous research work shown above, coordinate measuring machine (CMM) was used to get the coordinate points of runner blade profile rather than using XFLR5 software. Obtaining minimum angle of attack at all cross section of the runner blade to get optimized micro Kaplan turbine runner is not addressed. To overcome this drawback, research has been carried out in this paper by developing the runner blade using XFLR5 software in the blade profile geometry to fill the gap and carry forward the latest research.

CHAPTER THREE

DESIGN OF A MICRO KAPLAN TURBINE RUNNER

This chapter describes the design procedure of a Micro Kaplan turbine runner, i.e. to determine the runner dimensions. The process of geometry parameterization, measuring of design data's, detailed calculation of main dimensions of the runner geometry and draft tube and development of Kaplan turbine runner using the related empirical formulas are described in detail. Different empirical formulas, design steps, underlying assumptions, graphs and techniques are described in detail. Plan view of the runner assembly is also provided.

3.1Kaplan Turbine Runner

According to Alie Wube Dametew, the runner is the heart of the turbine and impacts design decisions about other aspects of the turbine. Water at high pressure is fed through the casing. The high-pressure water enters the runner inlet and flows through the area between four blades of the runner. Unlike in an impulse turbine, the reaction turbine directly uses water pressure to move turbine runner blades. The pressure difference produced between the two sides of blade creates the torque and finally mechanical energy in the form of rotation of runner [17]. The main runner dimensions to be designed which includes hub and tip diameter, blade angles, twist and spacing. Blades are responsible for capturing the most possible energy from the water. The runner in a Kaplan turbine is a very challenging part to design. The propeller shaped runner is mounted vertically with four blades. The length and number of blades can determine the turbine's rotational torque which can indirectly influence the hydraulic effect. It should be closely matched to your site characteristics. Careful machining makes a big difference in turbine efficiency.

3.2 Methodology

In order to solve problems, engineers follow and apply different procedure and principles based on the problem identifications. This section presents the methodology used to achieve objective of the thesis and is discussed as follow.

1. Start: need identification, problem definition

2. Perform literature review; identify site location, measuring basic design data's (fluid flow rate and gross head) from a specific site.

3. Select the type of turbine runner suitable for the site and design it using empirical formula.

4. Generate 3D model of the turbine runner and make its performance analysis using CFD.

5. Verify the CFD results with that of Dr. R.Khare similar work [8].

6. Make conclusion and recommendations

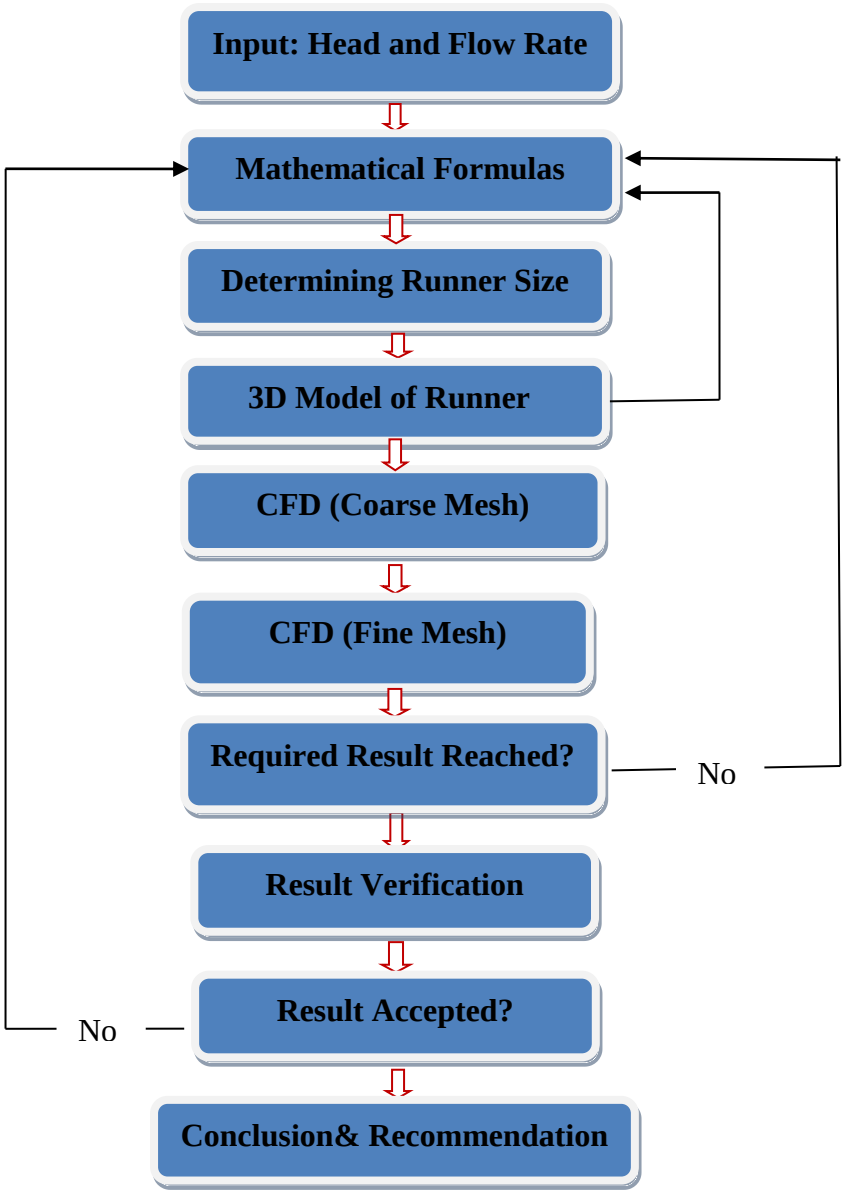

Figure 3.1: Design methodology flow chart

Fig.3.1 indicates the general design methodology chart of runner. The process started with measuring of basic input data's which are the head and fluid flow rate value available at the site selected. The mathematical formulas were used for the determination of runner size. It was changed to 3D model of runner to perform CFD analysis, if not return back and check the formulas. Verification with that of other similar research work was performed followed to CFD simulation results. When the requested conditions were fulfilled, write the conclusion and recommendation unless check the mathematical formulas.

3.3 Site Data

When assessing a micro-hydro site, one is interested in quantifying the site data, which is both the available gross head and fluid flow rate. The choice of the rotational speed (n) depends on the speed of the generator and type of the drive used. Since the site has not historical data's on fluid flow rate during field survey, the site data's are collected in March which is expected to have minimum value.

3.3.1 Over View of the Selected Site

Denkaka is found in Adda Woreda Oromia Zone. The site is located 15 km from Bishoftu town. It is geographically situated at East-South 34° from Modjo on the coordinate of 8.67°N, 39.03°E with an elevation of 1900 meters above sea level (source: Google earth). The river which flow near by the village has proved the capacity to generate a micro hydro potential during dry season.

As the result of measuring basic input data's of the selected site indicates, the available rate of fluid flow and gross head are $0.6 m^3/s$ and 3.125m respectively which has a capacity to generate 14.7Kw of net power. So, based on the selection criteria Micro hydro Kaplan turbine is selected for this study. Kaplan turbines are mainly used for low head and high flow rate applications [9].

3.3.2 Head Measurement Using Direct Method

There are various methods used to measure the head of a site. Direct height measurement method is one of them and because of its better accuracy; this method has been used to determine the site's head.

To measure head, instruments such as laser level, surveyor's transit, contractor's level on a tripod, or a sight level can be used.

The steps used to do the measurement are as follow:

a) Measure height of level using stick to determine head for each leg.

b) Subtract height of level from the stick

c) Repeat multiple steps from intake location to turbine location.

d) Add the head of each leg together to determine total head.

Table 3.1: Measurement of total head using direct height method

No	Measurement on stick (m)	Debth from water surface (m)	Head difference
1	2.5	1.3	1.2
2	1.65	1.0	0.65
3	1.2	0.58	0.62
4	1.0	0.40	0.60
5	0.305	0.25	0.055
Total head difference = 3.125			

3.3.3 Water flow- rate Measurement

As the flow rate of any river varies during a year, it is preferred to have a full hydrological record of the river, in order to determine a base flow rate data that can be used for turbine runner design. If such information is not available, the flow rate should be measured directly for at least a year. A once off instantaneous flow rate measurement is usually of little use, since nothing is known on the variation of the flow rate during the rest of the year.

The historical flow rate data of the river is not available (office of water and irrigation, Adda distinction); hence the flow rate was measured in March 2016, the month in which minimum flow rate is expected. There are various methods that can be used to measure the flow rate of a river, but only the methods discussed below were used for Water fall.

To determine the flow rate, the velocity of the water and the cross-sectional area of the river at the point where the flow rate is being measured need to be known. According to [18] the flow rate of the river can be determined using eqn.3.1

$$Q_r = V_r * A_r \quad (3.1)$$

Where:

Q_r Is fluid flow rate of the river

V_r Is velocity of the fluid flow of river

A_r Is cross-sectional area of the river.

The easiest way to measure the velocity of the water is, using the timing of a float, example a piece of leaf, over a certain measured length of the river as illustrated in Fig. 3.2. As can be seen from the figure, due to surface friction, the velocity profile of the moving water is not constant. It is therefore necessary to make velocity measurements at various points across the width of the river, average these measurements and then multiply the result by a certain correction factor, to obtain the mean velocity of the flow, based on the surface velocity of the float [13, 19]. Various correction factors are given in Table 3.2.

The cross-sectional area of the river can be calculated once the shape of the river bed has been established. To establish this shape, the depth of the water must be measured at various points over the width of the river. These water depth measurement points should preferably be at the same successive points where velocity measurements were made. According to [18] the cross-sectional area is then calculated from the equation given below.

$$A_r = h_{ave} * b \quad (3.2)$$

Where:

A_r Cross-sectional area of the river

h_{ave} Average height of water in the river or stream (m). ($h_{ave} = \sum h/k$)

b Width of the river (m)

$$A_r = b \times \frac{h1+h2+h3+\cdots h_k.}{k}\ m^2 \quad (3.3)$$

$$\text{Surface speed, } V_{rs} = \frac{L}{t}\ (m/s) \quad (3.4)$$

Where:

V_{rs} Average surface speed of the river

L Length over which float is timed [m]

t Time taken in (second)

k number of measurements

The velocity of fluid flow of river is the product of correction factor (C_f) and surface speed [18]

$V_r = C_f \times V_{rs}$ (m/s)

Table 3.2: Correction factors to obtain the velocity of flow rate in a river [20, 16].

River Type	Correction factor
Smooth, rectangular concrete channel	0.85
Large, slow clear stream (A> $10m^2$)	0.75
Small, slow clear stream (A < $10m^2$)	0.65
Shallow turbulent stream (debth,0.5m)	0.25-0.45

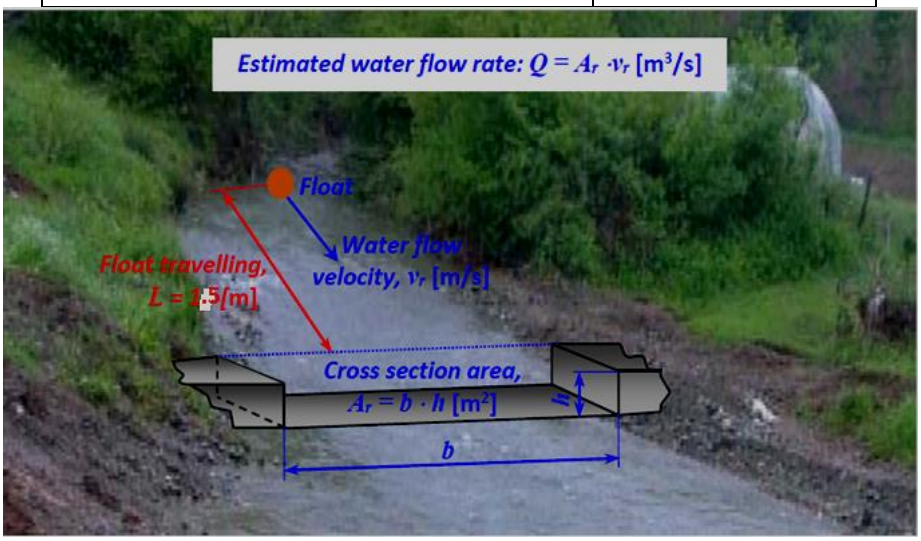

Figure 3.2: Measuring of water flow-rate by the floating approach [20].

The average flow rate for the measuring period in March is about $0.6m^3/s$. This value is the lowest flow rate that exists in the river as it was measured during late summer.

Table 3.3: Flow rate Measurements Using the Velocity-Area Method

Measuring point	Debth,[m]	Width b,[m]	Length over which float is timed [m]	t [s]	speed of particle [m/s]
1	0.43	2.09	1.5	1.02	1.47
2	0.40			1.01	1.48
3	0.45			1.02	1.47
4	0.38			1.03	1.46
5	0.42			1.01	1.47
Average debth = 0.41					
Average surface speed of the fluid flow of river, V_{rs} [m/s] = 1.47					

Crossectional area of the river, $\mathbf{A_r}$= 0.41*2.09 = 0.86$\mathbf{m^2}$ and

Velocity of the river, V_r = 0.45*1.47 = 0.7m/s

Q = V_r*A_r = $(C_f \times V_{rs} \times A_r)$ m^3/s = 0.45×1.47×0.86 = 0.6m^3/s

3.4 Conventional Design Methods

The conventional hydro turbine design methods, combined with hydraulic turbo machinery theory, permits the computation of the runner capacity and the preliminary design of the entire runner geometry. The first step in using conventional design method is problem definition. Efficiency, power, rotational speed, specific speed and runner blade angles are key geometric parameters in conventional design method.

3.4.1 Specific Speed

The specific speed constitutes a reliable criterion for the selection of a turbine. It is a determining factor for appropriate turbine speed [18]. This is more important to drive the correct gear ratio needed in producing the required generator speed for either charging the battery or providing directly to load. It is a dimensionless parameter and characterizes the hydraulic properties of a turbine in terms of speed and discharge capacity; it is based on simulated rules. The net head and discharge are also parameters used to determine the suitable type of turbine for the site selected. Turbines like Kaplan work efficiently at high fluid flow rate and low head. The selection of type

of turbine that is desired to run the generator of the hydro site is supported by tables, charts and graphs. Scientifically it is given as equation (3.5)

$$n_{QE} = \frac{n \times \sqrt{Q}}{E^{3/4}} \quad (3.5)$$

Where:

n_{QE} Specific speed of the turbine (-)

E specific hydraulic energy of machine (J/kg)

n rotational speed of the turbine (s^{-1})

Q volume flow rate (m^3/s)

The specific hydraulic energy of machine can be established with the following equation:

$$E = H_n * g \quad (3.6)$$

Where:

H_n Net head (m)

g Acceleration due to gravity (m/s^2)

$$H_n = H_g - \sum(\text{losses}) \ (m) \quad (3.7)$$

where:

H_g Gross head (m)

$\sum(\text{losses})$ Summation of head losses (m)

Head losses are a function of the penstock length, diameter, internal surface roughness, flow-rate, and the number and type of fittings between the intake and the turbine. For a straight penstock, friction is proportional to the velocity of the water and to the ratio of the penstock's length with respect to its diameter. The summation of losses in straight penstock and fitting loss is obtained the total head loss. This relationship is expressed mathematically by the Darcy equation (3.8)

$$h_{total} = h_{st.pipe} + h_{fitting} \quad (3.8)$$

Where:

h_{total} Total head loss

$h_{st.pipe}$ Head loss in penstock

$h_{fitting}$ Head loss in pipe fittings

$$h_{total} = f \frac{L}{D} \left(\frac{V^2}{2g}\right) + \sum k \left(\frac{V^2}{2g}\right) \quad (3.9)$$

Where:

f is friction factor

L length of penstock (m)

d inner diameter of penstock (m)

K is friction head loss coefficient

V fluid velocity (m/s)

g acceleration due to gravity (m/s2)

The first head loss that we considered is friction losses in the penstock. The friction factor (f) depends on the Renaldo's number (Re) and $\boldsymbol{\varepsilon}/d$, is specific to the material, construction of the pipe and the characteristics of the flow. The most widely used method of obtaining the friction factor is through the use of the Moody chart Fig.7.3 (Appendix). It shows the friction factor plotted against the values of Reynolds number (Re = $3.3x\boldsymbol{x}10^6$).

$$Re = \frac{V*d}{\nu} \quad (3.10)$$

Where:

V Velocity of water inside the penstock

d Inner diameter of penstock

ν Kinematic viscocity

According to Warnick (1984), the external diameter of penstock (D_p) for small hydro projects in terms of rated discharge (Q) were developed and are given as equation (3.11):

$D_p = 0.72\sqrt{Q}$ (3.11)

$D_p = 0.558m$

The penstock wall thickness (t) is also given by

$t = \frac{P*D_p}{2\sigma}$ (3.12)

Where:

P pressure with respect to gross head

σ Allowable stress

$t = \frac{\rho*g*h*D_p}{2*5.2x10^4} = \frac{998*9.8*3.125*0.558}{2*5.2x10^4} = 0.16m$

The inner diameter (d) of penstock is calculate by subtracting twice of wall thickness (2t) from external diameter of the penstock i.e

$d = D_p - 2t = 0.558 - (2*0.16) = 0.238m$

The velocity of water inside the penstock is also obtained from the relation of flow rate and cross sectional area as given below

$Q = A*V \Rightarrow V = \frac{Q}{A} = \frac{4Q}{\pi d^2} = \frac{4*0.558}{\pi(0.238)^2} = 12.5m/s$

$Re = \frac{12.5*0.238}{0.9x10^{-6}} = 3.3x10^6$

With a series of parametric curves related to the relative roughness of the penstock, the pipe roughness factor (ε) is obtained in the following Table 3.4

Table 3.4: Values of pipe roughness factor for various materials [17]

Material	**ε (mm)**
Drawn tubing,brass,glass,bituminous lining	0.0015
Commercial steel or wrought iron	0.046
Welded steel pipe	0.46
Galvanized iron	0.15
Concrete	0.3-3
Riveted steel	0.9-9

In our case, wrought iron is used for the work. Now when the pipe roughness factor is know it is simple to calculate the friction factor (f) as a function of f (ε/d, Re) using the moody chart. There are also certain losses that occur at the penstock entrance resulted due to the contraction and subsequent expansion of water streamlines flowing into the penstock. The third commonly encountered pipe fitting also induce losses in the system. Values of head loss coefficient for various pipe fittings is tabulated in Table 3.5

Table 3.5: Head loss coefficient for various pipe fittings [17]

Fitting	**$K_{fittings}$**
Gate valve (wide open)	0.19
Gate valve (half open)	2.06
Long radius bend	0.6
Short radius bend	0.9
T 9 through side outlet)	1.8
Smoothly curved contraction	0.05

According to Alie Wube Dametew [17] the total head loss can now easily be calculated by using the head loss coefficient for each entrance, pipe section and pipe material using equation (3.13). Assume smoothly curved contraction type of fitting is used for this work and change of

temperature is negligible. Now the total head loss is the sum of head loss due to friction in straight pipe and due to minor (fitting) loss this is given by (3.13)

$$h_l = (f\frac{L}{D}\frac{V^2}{2g}+\sum K\frac{V^2}{2g}) \quad (3.13)$$

According to Flotow (Micro Hydro Penstock Design, 2012) the length of the penstock is obtained from the relation given below

L = 10d = 10*0.26 =2.6m

$h_l = \{(f\frac{L}{D}+\sum K)\frac{V^2}{2g}\}$ m => $\{(0.014*2.6/0.6+0.05)*\frac{(11)^2}{2*9.81}\}$ m => h_l = 0.65m

Now the net head (H_n) = gross head (H_g) - ∑(losses) = (3.125 – 0.65) m ≈ **2.5m**

Using the net head value (H_n=2.5m), fluid flow rate (Q = 0.6m^3/s) and the turbine selection chart Fig.3.3, Kaplan turbine is suitable for the site selected.

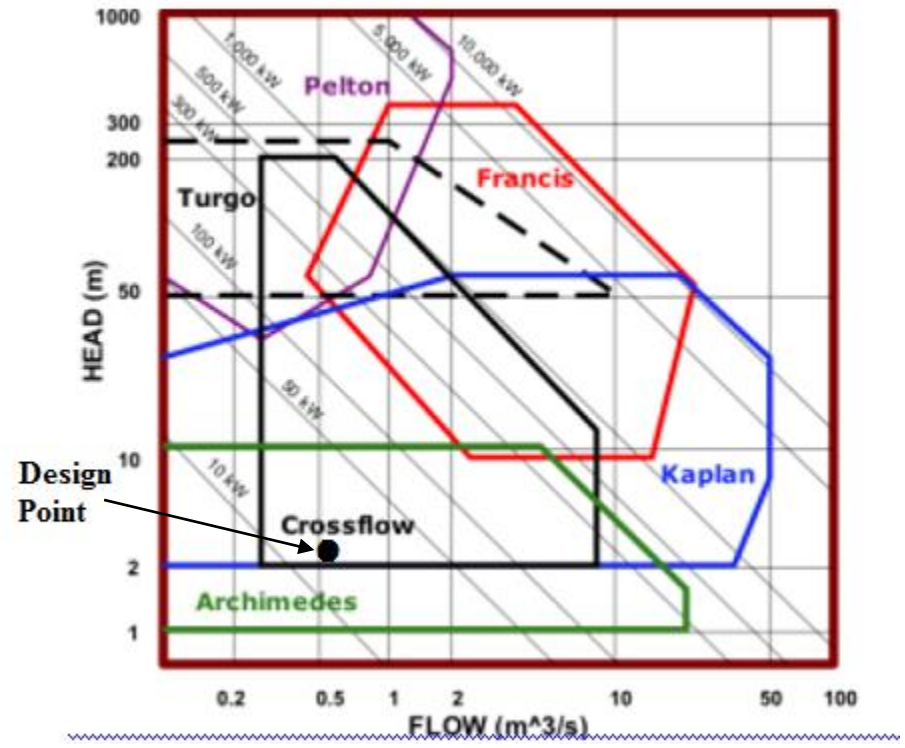

Fig. 3.3: Hydro Turbine Selection Chart [**Source**: net head application for micro hydro.com]

Synchronization Speed of Generator

Synchronous generator is used in most MHP systems because it has the ability to establish its own operating voltage and maintain frequency while it is operating in a remote location. In the low head hydroelectric power plants, standard generators should be installed. Therefore, rotational speed of the turbine which is directly proportional to its specific speed, fluid flow and net head is also important for the synchronization speed of generator that will be used in the scheme. Generators synchronization speeds for 50 Hz frequency are given in Table 3.6 with different number of poles.

Table 3.6: Generator synchronization speed (at f = 50Hz) [18]

# of poles	2	4	6	8	10	12	14	16	18	20	22	24	26
N (rpm)	3000	1500	1000	750	600	500	428	375	333	300	272	250	231

Now the standard value of speed of a turbine (n) = 600rpm≈ $10s^{-1}$ in which the frequency of the generated AC-50Hz is selected. Once the speed of a turbine is selected, the specific speed of the turbine is calculated using (3.14)

$$n_{QE} = \frac{n \times \sqrt{Q}}{E^{3/4}} \quad (3.14)$$

n_{QE} Specific speed (-)

n Rotational speed the turbine(s^{-1})

Q Volume flow rate (m3/s)

E Specific hydraulic energy of machine (J/kg)

$$\Rightarrow n_{QE} = \frac{10 \times \sqrt{0.6}}{(2.5 \times 9.81)^{3/4}} = \mathbf{0.7}$$

Now, the value of specific speed of the turbine is 0.7 which falls in the range of Kaplan turbine Table 3.7.

Table 3.7: Range of specific speed for each turbine [21]

Turbine type	**Specific Speed**
Pelton one nozzle	$0.005 \leq n_{QE} \leq 0.025$
Pelton n nozzle	$0.005\ n^{0.5} \leq n_{QE} \leq 0.025\ n^{0.5}$
Francis	$0.05 \leq n_{QE} \leq 0.33$
Kaplan, Propeller, bulb	$0.19 \leq n_{QE} \leq 1.55$

3.4.2 Power

According to Dilip Singh [22] a water turbine is a rotary machine that converts potential energy and kinetic energy of water into mechanical work. Thus the available theoretical hydraulic power available from a given head of water in exact proportion to the net head and the quantity of water available and can be calculated with the following equation:

$P_{hyd} = Q \times H_{net} \times \rho \times g$ watts (W) (3.15)

Where,

P_{hyd} = available/theoretical hydraulic power in watts (W)

H_{net} = the net head in meters (m)

Q = Flow rate in cubic meters per second (m^3/s)

ρ = density of water (kg/m^3)

g = acceleration due to gravity (m/s^2)

P = 0.6×2.5×1000×9.81(W) = 14.7kW

The Euler turbine equation relates the power added or removed from the flow, to characters tics of a rotating blade row. The equation is based on the concepts of conservation of angular momentum. Fig.3.4 shows the velocity triangles at the entry and exit of the turbine and is usually

drawn at the mean radius, since conditions change from hub to tip. The flow velocity is axial at inlet and outlet, hence w1= w2 = w.

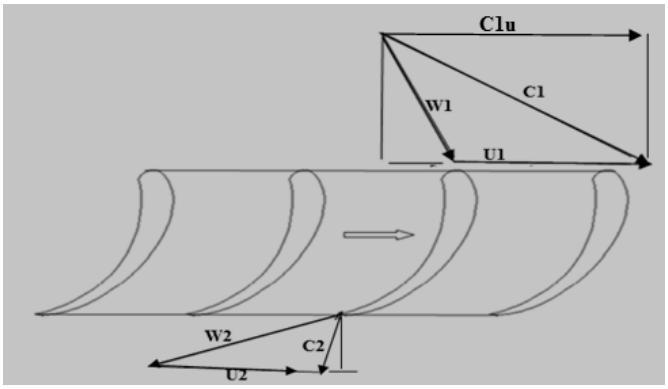

Figure 3.4: Velocity triangles at entry and exit of an axial flow Kaplan turbine runner blade

Acording to Abid. A.B. [24] the fluid velocity at the turbine entry and exit can be decomposed in to components, in the tangential and axial of the rotor and each velocity also produces their corresponding force. Out of those the tangential force only can cause the rotation of the turbine runner and produce work. The axial component force produces a thrust in the axial direction, which is taken by suitable thrust bearings. The power produced by the tangential force equals the product of the mass flow, tangential force and the tangential velocity at a mean radius of r. Considering the velocity triangles at entry and exit of the turbine, shown in Fig. 3.2 above and applying the concept of conservation of angular momentum, the initial and final angular momentum is calculated by the following equations (3.16) and (3.17) respectively

The initial angular momentum, $J_1 = \dot{m}(C_{u1}r)$ (3.16)

The final angular momentum, $J_2 = \dot{m}\,(C_{u2}r)$ (3.17)

Now, in rotational motion the rate of change of angular momentum is equal to the developed torque and is expressed as.

$T = \dot{m}(C_{u1}r \_ C_{u2}r)$ (3.18)

Where;

T The developed torque (N-m)

J_1 The initial angular momentum (kgm^2/s^2)

$\dot{m}$ Mass flow rate (kg/s)

u Tangential component of the absolute velocity at the entry (m/s)

J_2 The final angular momentum ($kg\ m^2/s^2$)

C_{u2} Tangential component of the absolute velocity at the exit (m/s)

r The mean radius (m)

Similarly the power developed in rotational motion is equal to torque times angular velocity and is expressed as eqn. (3.19)

$P = T\omega$ (3.19)

Where;

P power developed (kw)

ω Angular velocity of the turbine runner (rad/s)

$Power = \dot{m}\ \omega\ (C_{u1}r\ \_C_{u2}r)$ (3.20)

Since the turbine runner blade velocity, $U_1 = U_2 = U$ is the product of angular velocity (ω) and radius r, the rate of work done is calculated by the following eqn.(3.21)

$P = \dot{m}\ (C_{u1}U_1\ \_C_{u2}U_2)$ (Euler's Turbine Equation) (3.21)

$P = \dot{m}U\ (C_{u1}\text{-}C_{u2})$

Since Ethiopia uses a classification of hydropower systems which differs from other countries, the Ethiopian definitions as shown in Table 3.8 are used throughout this paper. Hence, using the results obtained above (eqn. 3.21) this paper lies under micro Kaplan turbine.

Table 3.8: Ethiopian hydropower classification. [Source: BÖLLI, FEIBEL 2008]

Terminology	Capacity limits	Unit
Large	>30	MW
Medium	10-30	MW
Small	1-10	MW
Mini	501-1000	kW
Micro	11-500	kW
Pico	<10	kW

3.4.3 Theoretical Hydraulic Efficiency

The potential energy of the water is converted to mechanical energy by the rotation of the turbine runner. This energy is transmitted by the shaft to the generator where it is transformed to electrical energy. Ability of the hydraulic turbine to transmit this potential energy of water to mechanical energy by rotation is measured by the efficiency of the turbine which is defined as

$$\eta_h = \frac{\text{power developed by the turbine runner}}{\text{power available at the entrance of the turbine}}$$

(3.22)

$$\eta_h = \frac{\dot{m}\, U\,(C_{u1} - C_{u2})}{\dot{m} g H} = \frac{U\,(C_{u1} - C_{u2})}{gH}$$ (Theoretical hydraulic efficiency equation)

3.4.4 Rotational Speed (n)

According to equation (3.23) the rotational speed of a turbine is directly linked to its specific speed, flow and net head. In the small hydro schemes standard generators should be installed when possible, so during turbine selection it must be considered that the generator is either coupled directly or through a speed increaser to the turbine, should reach the synchronous speed.

As given in Table 3.7. In our case the corresponding rotational speed (n) = 600rpm $\approx 10s^{-1}$ as turns per second is selected in such a way that the frequency of the generated AC is 50Hz.

Now, according [18] the rotational velocity (n) = $\frac{120f}{P}$ (3.23)

Where:

f = frequency

p = no of poles.

$f = \frac{600*10}{120}$ = 50Hz

Therefore, this value of rotational speed is optimal because it is synchronous to the generator speed Table 3.7: Thus, the turbine can be directly coupled to following.

3.4.5 Runaway Speed (n_{max})

The runaway speed is the maximum speed which the turbine can theoretically attain; it is achieved during a load rejection. Depending on the regulation of the Kaplan turbine, the following guidelines can be used to determine the runaway speed:

Table 3.9 Selection of Runaway speed [21]

Turbine Type	Runaway speed n_{max}/n
Single regulated Kaplan turbine	2.0 – 2.6
Double regulated Kaplan turbine	2.8 – 3.2

The turbine is supposed to work single regulated which means only the turbine runner blade is adjustable not the guide vane. Double regulated means both the runner blade and guide vane are adjustable.

Hence, n_{max} = 2.6*10 = 26 s^{-1} = 1500rpm arises.

3.5 Runner Design Procedures

Procedures are followed in the designing process of runner. After determining the runner design data and parameter, the preliminary sizes of the turbine runner are determined based on empirical formulas, assumptions and graphs. Therefore once the runner speed, specific speed and the design head are known, runner tip diameter, hub diameter and the height of hub are determined. Preliminary blade model can be formed.

3.5.1 Runner Tip Diameter (D_{tip})

According [18], the runner tip diameter D_{tip} can be calculated using eqn. (3.24)

$$D_{tip} = [84.5*(0.79 + 1.062* n_{QE}) * \frac{\sqrt{H_n}}{60*n}]m \quad (3.24)$$

$$=> D_{tip} = 84.5*(0.79\ 1.602*0.7) * \frac{\sqrt{2.5}}{60*10}$$

D_{tip} = 0.4m

3.5.2 Runner Hub Diameter (D_{hub})

The hub diameter (D_{hub}) can be calculated with the following equation (3.25)

$$D_{hub} = (0.25 + \frac{0.0951}{n_{QE}}) * D_{tip} \quad (3.25)$$

$$D_{hub} = (0.25+\frac{0.0951}{0.7}) * 0.4m$$

D_{hub} = 0.15m

3.5.3 Cavitation

In the fact that the vapor pressure of a liquid exceeds the hydrodynamic pressure of the liquid flow, a small part of the water changes into the vapor phase; this causes the formation of vapor bubbles in the liquid stream. The less the static pressure the more number of vapor bubbles also size of bubbles. Finally, the water carries the bubbles to a spot where the liquid pressure increases again. The vapor bubbles are not able to withstand the higher pressure and they

collapse in an imploding manner. This implosion releases very fast micro streams and pressure peaks of up to some hundred MPa occur.

In particular places in the working circuit of the hydro turbine there is decrease in pressure during passing of water through the flow-through line can lead to occurence of cavitation. Cavitation can be simply explained in the following manner: If in a continuous flow of liquid, the speed is raised from v1 to v2 kinetic energy rises and pressure drops from P_1 to P_2 . If the pressure drops below the critical level, liquid is transformed into steam which leads to local breaking of continuity of liquid and formation of cavities filled mostly with steam. In the case of a Kaplan turbine, the exit of the runner blade is quite susceptible to it. At parts with a high water flow velocity cavitation might also arise. Cavitation should be avoided because it has several negative effects on the turbine. First it decreases the efficiency and causes crackling noises. However, the main problem is the wear or rather the damage known as “pitting” of the turbine’s parts such as the blades. Cavitation does not just destroy the parts, chemical properties are also lost; for example, the material is not able to recover its protective layer which acts as protector against corrosion.

The suction head (H_s): is the head between the trailing edge of blade and trailing race; if the suction head is positive, the turbine runner blade is located above the trail water; if it is negative, the turbine runner blade is located under the trail water. To avoid cavitation, the range of the suction head is limited. The maximum allowed suction head can be calculated using the following equation.

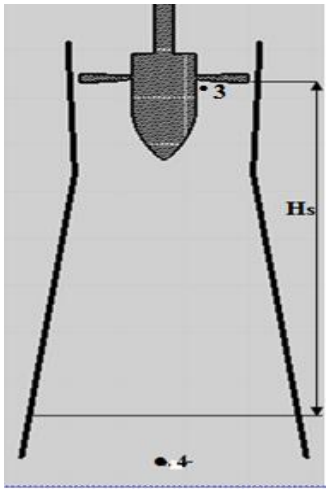

$$H_s = \frac{P_{atm} - P_v}{\rho * g} + \frac{C^2_4}{2 * g} - \sigma * H_n \text{ [m]} \quad (3.24)$$

Where:

P_{atm} Atmospheric pressure [Pa]

P_v Water vapor pressure [Pa]

ρ Water density [kg/m3]

g Acceleration of gravity [m/s2]

C^2_4 Outlet average velocity from turbine [m/s]

σ cavitation coefficient [-]

H_n Net head [m]

Figure 3.5: Sketch of 2D Kaplan turbine suction head

The value of cavitation coefficient (σ) is calculated using the formula given below. Thus the value of σ for the Kaplan turbine can also be established with the following equation [3.27]

$$\sigma = 1.5241 * n_{QE}^{1.46} + \frac{C^2_4}{2 * g * H_n} \quad (3.27)$$

The outlet velocity C_4 located at the outlet of the turbine draft tube, can be calculated using the turbine discharge and draft tube diameter as given below.

$$Q = A * C_4 \Rightarrow C_4 = \frac{Q}{A} \quad \text{but } A = \pi \frac{D^2}{4} = \pi \frac{(0.65)^2}{4} = 0.329 m^2$$

$$C_4 = \frac{0.6}{0.329} = 1.83 m/s$$

Now, the value of 1.83m/s outlet velocity was used to calculate the cavitation coefficient. The vapor pressure depends on the water temperature. The temperature of Modjo reaches to a maximum of 26°C in the summer. Since the vapor pressure increases with higher temperatures the vapor pressure at 26°C is relevant for the cavitation calculation. At a water temperature of 26°C, the vapor pressure is 3363.8 Pa (Appendix, Table 7.1). The altitude of the selected site is 1920m above sea level; the atmospheric pressure at sea level is 101300 Pa.

Hence, a maximum suction head of -2.3m results from equation (3.28). As long as the chosen suction head is below the established suction head no cavitation occurs. There fore, a suction head of 0.625m < 2.3m is arbitrarily chosen [26, 27].

The pressure at the trailing edge of the blade is calculated as follow.

$$\frac{P_3}{\rho} + \frac{C^2{}_3}{2} + gH_s - gh_f = \frac{P_{atm}}{\rho} + \frac{C^2{}_{atm}}{2} + h_{atm} \qquad (3.28)$$

Where:

P_3 Pressure at trailing edge of blade

C_3 Velocity at trailing edge of blade

h_f Head loss in draft tube

$P_3 = P_{atm} - \rho(\frac{C^2{}_3}{2} - gH_s) = 101300pa - 1000(15.43 - 9.81* - 2.3) = 30934pa$

Hence, cavitation will not occur since $P_3 > P_v = 30934pa > 3363.8pa$

3.5.4 Design of Runner Blade

Development of the complex shaped three dimensional blades is very essential to proceed further for optimization of the blade profiles by utilizing the computational fluid dynamics analysis. For this purpose, blade profile of NACA 2412 is used to create the 3D solid model of runner blade and is obtained from XFLR5 Software using number of digit and panel as input and the output is the shape and coordinate pointes. It is accurate and reliable. NACA 2412 is slow speed airfoil; this airfoil is used in single engine like Cessna 152 airplane [28] and then is suitable for micro hydro turbine. The Profile geometrical data was developed in the form of coordinate points in x-axis, y-axis and z-axis. Appendix Table 7.2

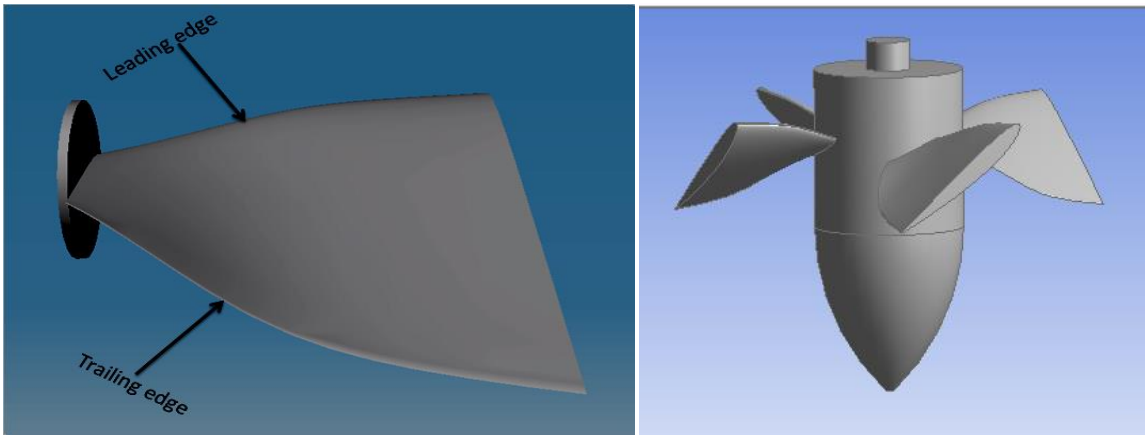

Figure 3.6: Plan view of runner blade (left) and turbine runner (right)

The design of the blade does not just depend on the stress analysis; several other factors play significant roles as well. The leading edge is thicker than the trailing edge for a streamlined flow. Furthermore, the blade should to be as thin as possible to improve the cavitation characteristics; it is thicker near the hub becoming thinner and thinner towards the tip. In addition, the blade has to be twisted on the basis of the tangential velocity

3.5.4.1 Twist of the Blade under Ideal Circumstances

The velocity triangles, which occur on the runner blade and the velocities of fluid flow is decomposed in to different velocity components, play a significant role in determining blade twisting Fig. 3.4.

When a cylindrical cut is set at the runner and the cut is developed into a drawing pane, a grating like that shown in Figure 3.6 occurs. Velocity triangle 1 occurs directly before the grating and the velocity triangle 2 occurs directly after the grating. The meridian components w1m and w2m are equal. The medial relative velocity can be determined via the average of w1 and w2 and its direction is specified due to the angle $\beta\infty$. Value t represents the grating partition and value l denotes the chord.

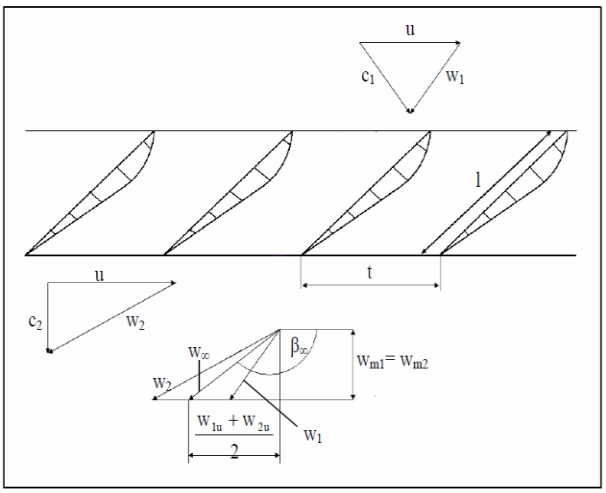

Figure 3.7: Grating [9]

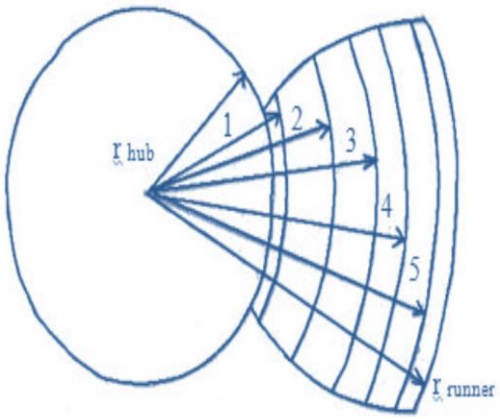

Figure 3.8: Five Sections of the Blade [9]

To define the twisting of the runner blade, determine first the six different diameters of the blade using velocity triangles, next the angle β∞, chord length of each radius and finally make lofting which gives conclusions on the twisting of the blade. Table 3.10 shows the velocities and the significant angles of the velocity triangles for each of the diameters and was tabulated using the equations described below [18].

For section I $r_1 = \frac{d}{2} + 0.015D$

For section III $r_3 = \frac{D}{2}\sqrt{\frac{1+(d/D)^2}{2}}$

For section II $r_2 = r_1 + \frac{r_3 - r_1}{2}$

For section V $r_5 = \frac{D}{2} - 0.015D$

For section IV $r_4 = r_3 + \frac{r_5 - r_3}{2}$

$U = \pi * n * d$ (3.29)

$c_u = H_\infty * \frac{g}{u}$ (3.30)

$w_u = c_u - u$ (3.31)

$$w_m = \frac{Q}{A} \quad (3.32)$$

$$W = \sqrt{{w_u}^2 + {w_m}^2} \quad (3.33)$$

$$w_{u\infty} = \frac{w_{u1}+w_{u2}}{2} \text{ and } w_{\infty} = \sqrt{\frac{{w^2}_{u\infty} + {w^2}_{m}}{2}} \quad (3.34)$$

$$\beta_{\infty} = 90 - \tan^{-1}\left(\frac{w_{u\infty}}{w_m}\right) \quad (3.35)$$

Where:

r diameter of the partial blade [m]

U The tangential velocity of the blade [m/s]

c_u The tangential velocity of the fluid flow [m/s]

w_u The tangential relative velocities [m/s]

w_m The relative velocity in meridian direction [m/s]

W The relative velocity at the middle of the blade [m/s]

$w_{u\infty}$ The relative velocity in the tangential direction [m/s]

β_{∞} The angle at the middle of the blade with horizontal [degree]

n rotational speed

d runner diameter

Table 3.10: Details of the theoretical runner design

Symbol	d_{hub}	I	II	III	IV	D_{tip}
d (m)	0.15	0.162	0.23	0.302	0.388	0.40
U(m/s)	4.7	5.08	7.22	9.48	12.18	12.56

c_{u1} (m/s)	5.53	5.11	3.60	2.74	2.13	2.07
c_{u2} (m/s)	4.90	4.53	3.18	2.42	1.89	1.83
w_{u1} (m/s)	0.51	-0.26	-3.83	-6.90	-10.17	-10.61
w_{u2} (m/s)	0.2	-0.58	-4.04	-7.06	-10.29	-10.73
$w_{u\infty}$(m/s)	0.35	-0.42	-3.93	-6.98	-10.23	-10.66
w_m (m/s)	5.55	5.55	5.55	5.55	5.55	5.55
w_1 (m/s)	5.57	5.55	6.74	8.85	11.58	11.97
w_2 (m/s)	5.55	5.58	6.86	8.98	11.69	12.08
w∞ (m/s)	3.93	3.94	4.8	6.3	8.23	8.5
β∞(degree)	86	94	125	141	151	152
(180- β∞)	94	86	55	39	29	28

The angles however, are not 100% accurate. To get the exact blade angles of twisting, the "Tragflügle theory" has to be considered. According to the "theory" a lifting force F_l applies at the blades of the runner due to the configuration of the parallel stream and the circulation stream, which occur at the blade. Hence, values such as the lift coefficient (C_L), drag coefficient (C_D) and the angle of attack (δ) also play a significant role in the design of the blade. These coefficients can be determined via experimental tests. Using these results the chord and the exact twisted of the blade can be determined. The following steps can be used to determine the blade's main characteristics.

Step 1: With the following equation, the lifting coefficients for each radius are determined [9]

$$C_L = \frac{{w_2}^2 - {w_\infty}^2 + 2*g\,[\,p_{atm} - H_S - P_{min} - \eta_h * \frac{{c_3}^2 - {c_4}^2}{2*g}\,]}{k * {w_\infty}^2} \qquad (3.36)$$

Where:

w_2 Relative velocity after the grating

w_∞ Merdial relative velocity

P_{atm} Atmospheric pressure

H_S Suction head

P_{min} Minimal water pressure (assumption)

η_h Hydraulic efficiency

C_3 Velocity after the runner

C_4 Average outlet velocity (assumption = 2m/s)

K profile characteristic number

Almost all the values of the equation are known either from previous section or they can easily be established. The other values have to be assumed where a range for these values is given. Using the ranges given in book the values are as follows:

P_{min}= 2 → 2.5(atm)

η_h = 0.80 →0.91

K = 2.6 → 3.0

Here:

$$C_3 = \frac{Q}{A_3} \Rightarrow A_3 = \frac{\pi * D^2_e}{4} = \frac{0.28^2}{4} * \pi = 0.062\ m^2$$

$$\Rightarrow C_3 = \frac{Q}{A_3} = \frac{0.6}{0.062} = 9.7 m/s$$

Step 2: When the lifting coefficient is known, the ratio of chord length to blade partition (l/t) can be established as follows [9]:

$$\frac{l}{t} = \frac{g * \eta_h * H}{w_\infty^2} * \frac{c_m}{u} * \frac{\cos\lambda}{\sin(180 - \beta_\infty - \lambda)} * \frac{1}{C_L} \quad (3.37)$$

Where:

l Chord length

t Blade partition ($t = \frac{2\pi r}{z}$)

z Number of blades

g Acceleration of gravity

η_h Hydraulic efficiency

H Gross head

cm Meridian velocity

U Tangential velocity

$(180-\beta_\infty)$ Inflow angle

The angle of slip (λ), which is formed on blade due to lift and drag forces, has to be assumed; the range for the assumption is as follows:

$\lambda = 1.0°- 3.0°$

Using this assumption, an approximate value of the ratio chord length to blade partition (l/t = 0.17) can be established Table 3.11.

Step3: The chart in the following figure gives information on the drag coefficient (C_D), lift coefficient (C_L) and angle of attack (α) for the selected NACA 2412 profile with Re = $3.1x10^6$.

Using Figure.3.7we can determine the values of angle of attack (α) and drag coefficient (C_D).

Experimental measurements on the NACA 2412 Airfoil

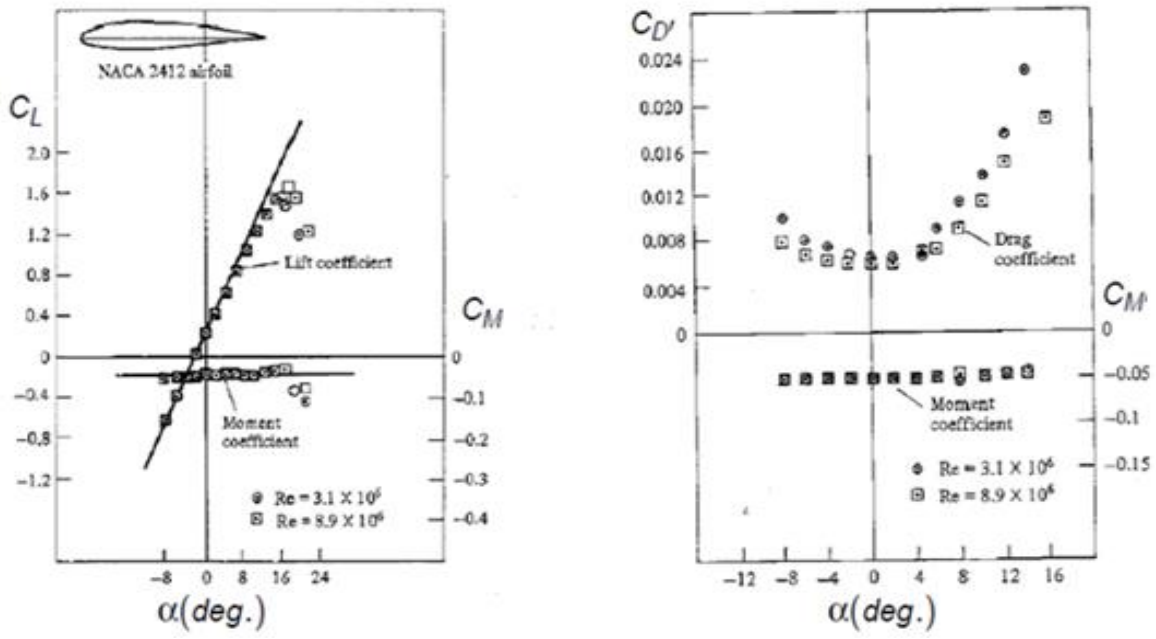

Figure.3.9: Graph of $C_L v_s \alpha$ and $C_D v_s \alpha$ [**source**: www.experimental measurement NACA Airfoil.com]

Step 4: With the following equation, the angle of slip can be calculated [18]

$$\lambda = \arctan\left(\frac{C_D}{C_L}\right) \tag{3.38}$$

It has to be checked whether the assumed angle of slip and the calculated angle of slip are similar or not. If the difference is too great, the procedure of the calculation has to be repeated using the angle of slip calculated. Steps 2 to 4 must be repeated until the angles of slip do not change any more. When the angle λ is fixed, it can be assumed that the last calculated values of Steps 2 to 4 are accurate enough, and then ratio l/t can be determined.

Step 5: Follow the above steps to fill the given Table 3.11 below using the blade profile 2412.

Table 3.11: Characteristics of blade at different diameter from hub

d (m)	0.15	0.16	0.23	0.30	0.388	0.4
t (m)	0.11	0.13	0.18	0.23	0.30	0.31
C_D	0.007	0.005	0.006	0.006	0.007	0.007
C_L	0.56	0.5	0.4	0.4	0.43	0.43
λ	1	1	1	1	1	1
$\alpha(deg)$	8	6	5	4	3	3
l/t	0.20	0.25	0.23	0.20	0.17	0.17
l (m)	0.022	0.032	0.041	0.046	0.051	0.053

To get the accurate blade twisting angle, the angle of attack (α) has to be subtracted from the angle (180-β∞) and the outcome of this is shown in Table 3.12.

Table 3.12: Angle of the twisted blade

d(m)	0.15	0.162	0.23	0.302	0.388	0.4
(180 - β_∞- α)	86	80	50	35	25	24

3.5.5 Design of Draft tube

The draft-tube is a pipe of gradually increasing area which connects the outlet of the runner to the tail race. It is used for discharging water from the exit of the turbine to the tail race. This pipe of gradually increasing area is called a draft-tube. The hydraulic characteristics of any draft tube depend on its shape, dimensions and the flow pattern at its entrance. Straight conical draft tube is the simplest type of draft tube and it has excellent hydraulic characteristics (Carija Z., Mrsa Z. and Dragovic). This draft tube has been eventually used for small and medium size vertical turbines. The cone angle is not to exceed 6°(Sumeet J.Wadibhasme, Prof. Shailendra Daf, 2016). For greater value of the cone angle it is seen that the flowing body of water may not touch the sides of the draft tube (Leaving the boundary. The detail dimensions of the draft tube at the flange angle which is approximately equal to a 6 degree are as below.

3.5.5.1 Length of Draft tube (Y)

According to [18] the length of draft tube (Y) is described as

$$Y = (2.5 \text{ to } 3)\, D \tag{3.39}$$

Where:

Y length of draft tube (m)

D Tip diameter (D = 0.4m)

Y = (3*0.4) m = **1.2m**

3.5.5.2 Outlet Diameter of Draft tube (D_{outl})

$$D_{outl} = D + 2Y \tan\alpha \tag{3.40}$$

$$= 0.4m + 2*1.2 (\tan 6)\ m$$

$$= 0.652m$$

D_{outl} = **0.652m**

CHAPTER FOUR

CFD ANALYSIS OF THE KAPLAN RUNNER

4.1 Introduction

This chapter provides a detail description to the CFD analysis of 3D model of Kaplan turbine runner to perform further evaluation of the turbine runner performance. The basic characteristic features of the runner we wanted to analyze by CFD simulation are principal dimensions of the turbine runner like tip diameter (D_{tip}= 40cm), hub diameter (D_{hub}=15cm), power input (p=14.7kw) and runner speed (n=600 rpm). The designed 3D runner geometry is imported to ANSYS-CFX for simulation to evaluate power output and efficiency of the runner. Meshing of the runner was done in ANSYS-CFX package. ANSYS-CFX solution flow chart (Fig.4.1) given below is used for CFD simulation of the designed 3D model of Kaplan turbine runner.

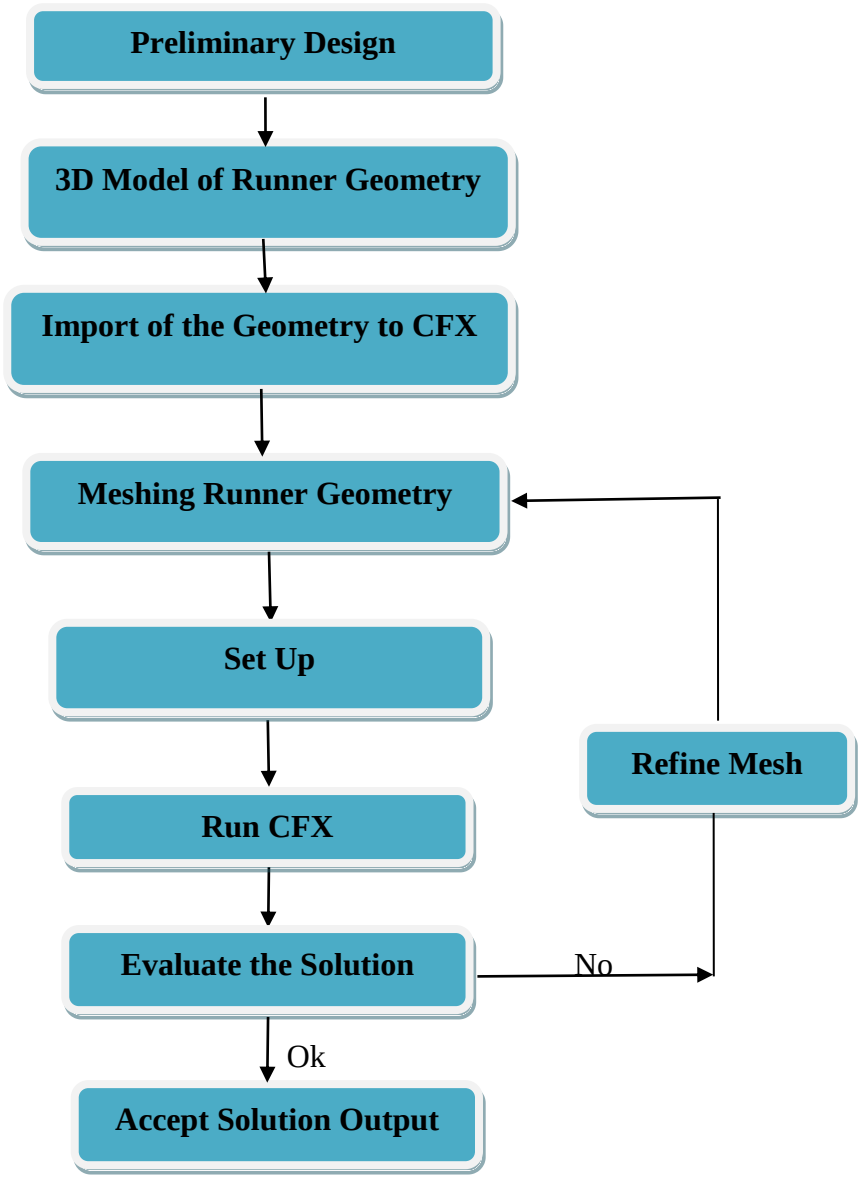

Figure 4.1: CFD simulation flow chart

There are five key modules displayed in section 4.4 are used to perform a complete work flow for one simulation towards improving the performance of the 3D model of Kaplan runner followed objective and challenges of CFD analysis. Finally, results obtained from CFD simulation are presented on the next chapter.

4.2 Objective and Challenges of CFD Analysis

The main objective is to establish the analysis of Kaplan turbine runner using CFD to predict the torque applied to a non-stationary runner, subject to a high flow velocity, to achieve an optimum performance of the runner like its output power and efficiency. When dealing with non-stationary fluid domains, the numerical analysis itself will be transient.

The main challenges regarding this analysis are:

• Large domain (three-dimensional)

• Transient simulation

• Complex mesh/grid (CFD)

• Stationary and rotating domains

4.3 Methodology

The designed 3D model of the runner was imported to the ANSYS Design Modeler. Figure 4.1 shows the structure of the 3D model created for CFD analysis. The turbine runner is centered inside the turbine casing for the CFD analysis.

CFD was chosen over the entire runner analysis. The computational domain is defined by the rotating domain and stationary domain. The rotating domain containing the blades. Fig.4.1 is in the initial position. From then on, this domain rotates inside the stationary domain along to z-axis. When modeling the fluid domain, it is important to make sure that the fluid flow is fully developed before interacts with the runner blade. The computational domain has two parts which are three dimensional bodies where the governing equations solved the movement of water.

4.3.1 Governing Equations

There are a very large number of CFD codes and programs available, as well as the possibility of creating a new one for a specific purpose. The different sets of equations are the conservation form of the Navier-stokes equations shown as below are the governing equation solved for transient and incompressible turbulence flow behavior prediction.

1. The continuity equation (4.1)

$$\frac{\partial \rho}{\partial t} + \nabla.(\rho v) = 0$$

2. Newton's second law of motion ($\sum \vec{F} = m\vec{a}$) (4.2)

x- Component: $\frac{\partial}{\partial t}(\rho u) + \nabla.(\rho u\vec{V}) = -\frac{\partial p}{\partial x} + \frac{\partial \tau_{xx}}{\partial x} + \frac{\partial \tau_{yx}}{\partial y} + \frac{\partial \tau_{zx}}{\partial z} + \rho f_x$

y- Component: $\frac{\partial}{\partial t}(\rho v) + \nabla.(\rho v\vec{V}) = -\frac{\partial p}{\partial y} + \frac{\partial \tau_{xy}}{\partial x} + \frac{\partial \tau_{yy}}{\partial y} + \frac{\partial \tau_{zy}}{\partial z} + \rho f_y$

z- Component: $\frac{\partial}{\partial t}(\rho w) + \nabla.(\rho w\vec{V}) = -\frac{\partial p}{\partial z} + \frac{\partial \tau_{xy}}{\partial x} + \frac{\partial \tau_{yy}}{\partial y} + \frac{\partial \tau_{zy}}{\partial z} + \rho f_z$

Where:

U, V and W designates velocity components, P designates pressure, ρ designates flow density and τ designates stress tensioner, $\vec{V}$ designates unit vector and t designates time.

Thus different sets of equations are the conservation form of the Navier-Stokes equations for viscous flow as set out in (Anderson, 1995). These are the fundamental equations that allow CFD programs to numerically analyze and predict the fluid flow and include important aspects such as friction and thermal conduction.

The runner geometry is placed inside the stationery domain, and the volume of this geometry occupies is subtracted from the stationery domain. The result is a hollow tube which takes the shape of runner geometry. This method is used to simplify the structure for CFD analysis during simulation. Next to that verification of CFD simulation results was performed using that of V.Chandrakar and R.Khare research work [8]. If there was not good agreement between the two, we can return back and check the runner size unless we wrote the conclusion if the runner performed a good performance.

4.4 Work Flow

A complete workflow for one simulation is presented in this section. The five key modules listed below are necessary to be able to set-up and complete the work flow of runner CFD analysis.

1. Geometry creation using Computer Aided Design (CAD)

2. Mesh creation – subdividing the flow domain into smaller grids

3. Physical set up – setting the boundary conditions

4. Running the solver – where the PDEs governing the flow through the machine are solved numerically.

5. Post processing – viewing the results of the solver through graphs and images of fluid flow. Fig 4.2 depicts the ANSYS Workbench project layout used for CFD analysis of runner.

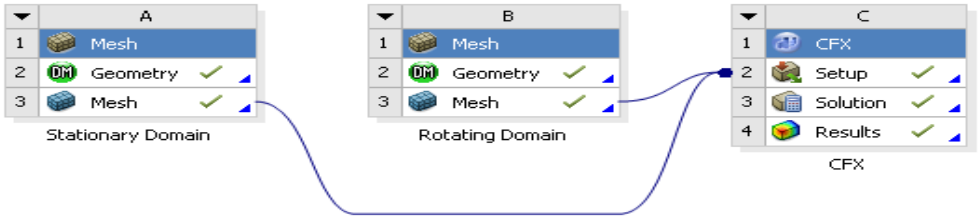

Figure 4.2: Project layout in ANSYS Workbench.

4.4.1 Geometry Creation

The designed Kaplan runner geometry was created using a combination of two CAD software packages normally, solid work and ANSYS Design Modeler. The geometry creation can be split into major sections

4.4.1.1 Creating Turbine Runner and its Draft tube

Primarily solid work was used to create the turbine runner geometry. Initially XFLR-5 software was used to get the co-ordinates of the NACA 2412 aerofoil series (appendix: Table 7.2) for different chord lengths at different radial positions and exported in to Microsoft excel which is saved as (.dat) format. Once, the setup in both excel and solid work is done, we exported the coordinates in to Generative shape design work bench of solid work and using the tools available there we were able to create the partial blades having different chord lengths Fig. 4.3a and then was made a loft to get 3D model of turbine runner blade Fig.4.3b. The size of the hub, which determined in chapter three, was changed to 3D model geometry Fig.4.3c. Finally complete

assemblies of runner components were performed to get 3D CAD model of the turbine runner shown in Fig. 4.3d below:

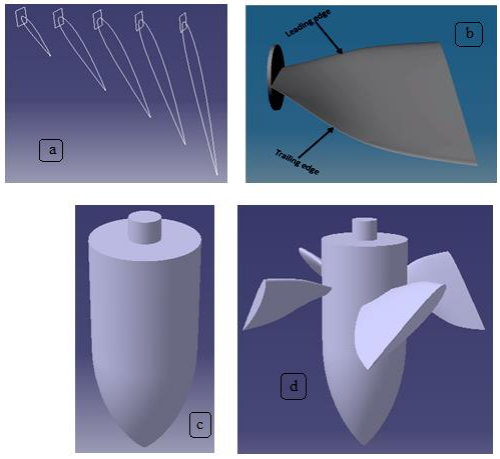

Figure 4.3: CAD model of Kaplan turbine runner

Secondly, the dimensions of the cone type daft tube were calculated using the empirical formulas which were done in chapter three sections 3.4.6 and the 2D and 3D CAD model geometry of it is created in ANSYS work bench (Fig. 4.4) shown below.

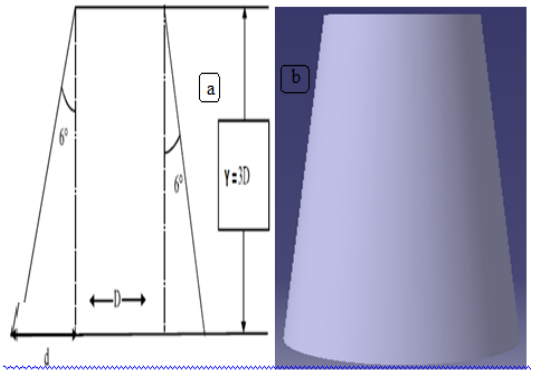

Figure 4.4: CAD model of cone type draft tube: a) 2D b) 3D

Figure 4.5 depicts the complete 3D CAD drawings of both the rotating and stationary domain which was modeled separately and assembled here to show their relative initial positions and was saved as (.stp). The complete turbine runner file was imported in to ANSYS Design modeler.

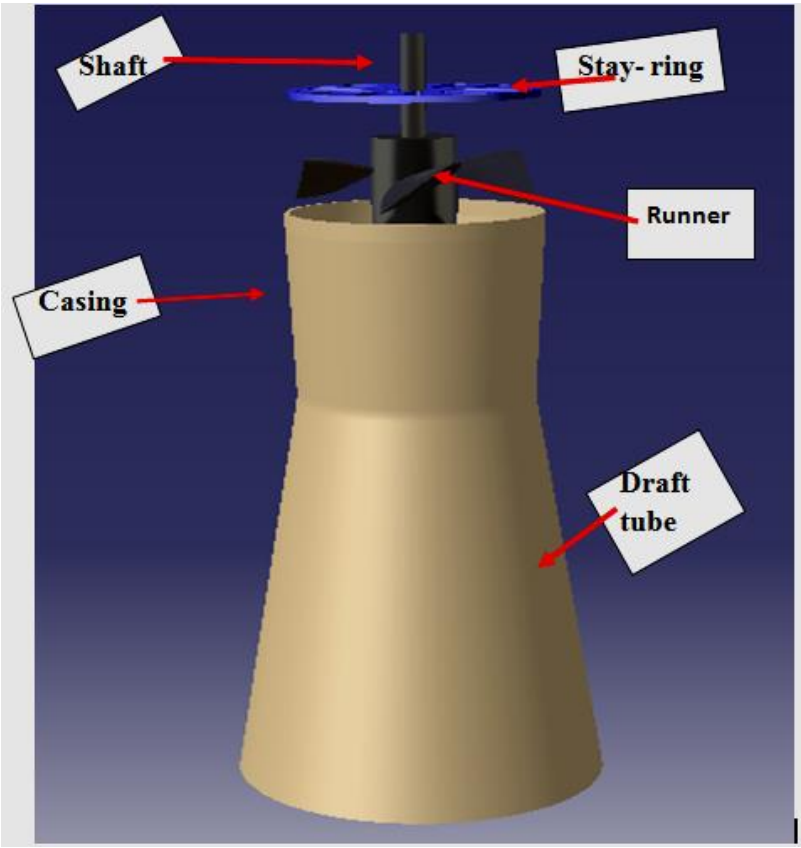

Figure 4.5: 3D CAD model geometry of runner and its draft tube

Analyzing of Flow Domain

The final phase used to prepare the flow domain to be analyzed was to effectively subtract the turbine runner from the casing and draft tube. This was carried out using the Boolean subtract feature. By doing this, it effectively creates the flow domain to be analyzed. The imprint left from the subtracted geometry was performed a named selection and will later be used to represent the runner model. As the 'filled' space represents the fluid, the empty section will be treated as the rotating runner wall

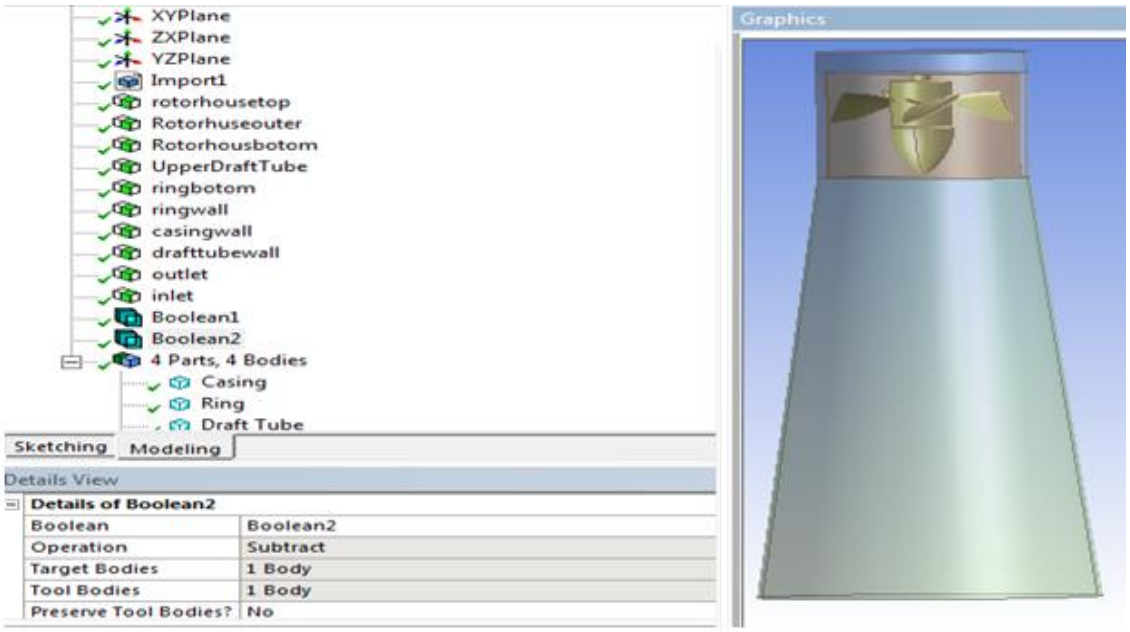

Figure 4.6: Boolean operation between the runner and casing on the rotating fluid domain

4.4.2 Mesh Creation

CFX is a mesh based CFD technique that uses Eulerian fluid flow field specification. It discretises the domain using cell-vertex numeric's (finite volume elements).When working with ANSYS Meshing 15.0, one should be aware of that the order one applies sizings, inflations etc. has an impact on the success of mesh generation. As shown on Figure 4.2, the meshing of the fluid domain was divided in two meshing components, one for the stationary domain and one for the rotating domain. The main reason for this was that the rotating domain was meshed with an advanced size function, while the stationary domain did not use this feature.

The construction of a good quality mesh is vital for successful and reliable CFD analysis. The role of the mesh is to decompose the flow domain into small control volumes called cells or elements, in a process called discretization (Kuzmin, 2015). CFX uses a cell vertex method where the vertices of the elements are nodes.

The governing equations are solved numerically and by iteration at the nodes or elements until convergence is reached to numerically solve the fluid flow. Convergence is achieved when the

governing equations (the mass and momentum) residuals have been solved to the required tolerance (Kuzmin, 2015).

4.4.2.1 Rotating Domain Mesh

The rotating domain was meshed with the advanced size and consisted of 1.4 million mesh elements and 0.27 million nodes. The mesh was tetrahedral element. The inflation layers shown in Fig. 4.7 were applied on the surfaces of interest both at the wall and where the surfaces of the hub and blades interact with the fluid flow.

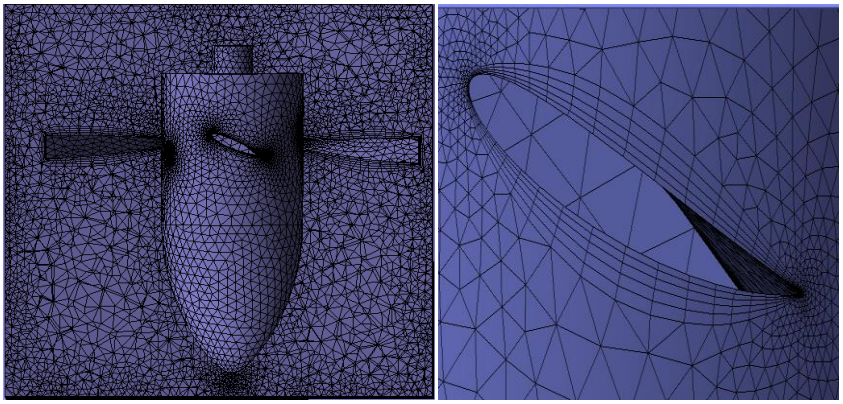

Figure 4.7: Rotating domain mesh (left) and inflation layer (right)

In the following section different 2D region will be given specific name that would be later used in boundary condition and value setting in the solver. In the rotating part of the flow domain (Rotor) 2D regions are named such as Rotor top, Rotor bottom and Rotor outer.

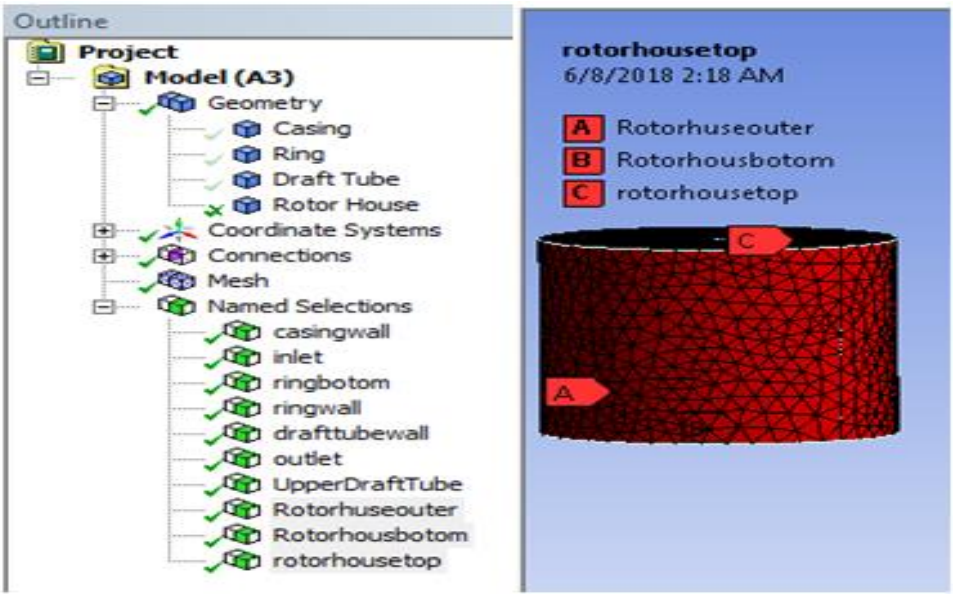

Figure 4.8: 2D regions naming at the interface between the two domains

4.4.2.2 Stationary Domain Mesh

The stationary domain was meshed with the advanced size function turned off and consisted of 0.021 million mesh elements and 0.0048 million nodes. All the elements were hexahedral and the sizing was controlled depending on the flow direction that was easily predictable in this domain. The skewness factor describing the quality of a hexahedral mesh was 0.7. Fig. 4.9 presents an image of the stationary domain. ANSYS Meshing 15.0 actually does a great job meshing the large part automatically. Stationary fluid domain consists of the casing and the draft tube coupled together and 2D regions in this case are named like inlet, wall and outlet.

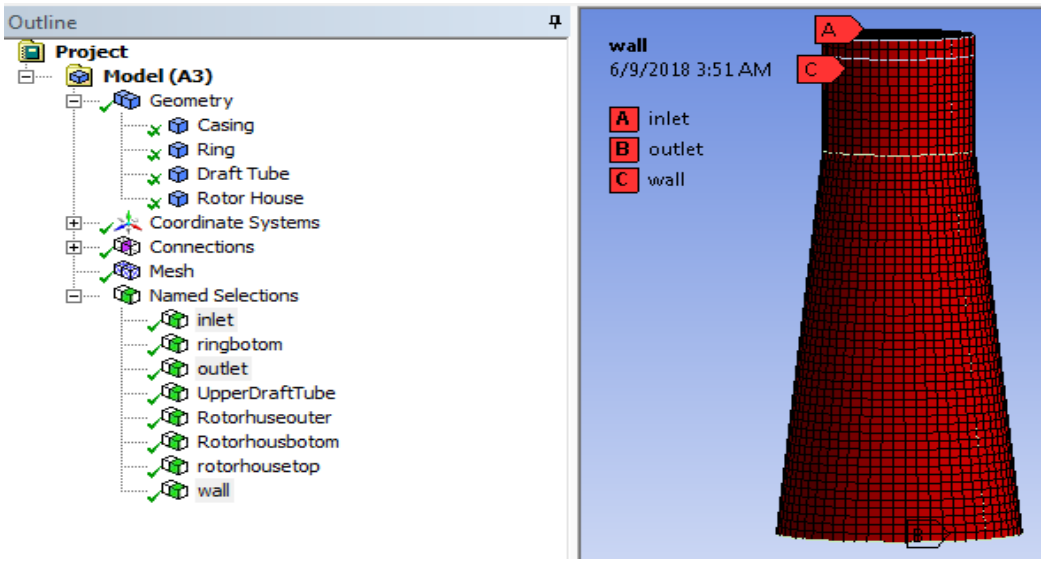

Figure 4.9: Naming of 2D regions on the stationary domain

4.4.3 Physical Setup

In a problem setup of a CFD modeling stage, important activities like selection of the appropriate transport equation, physical models such as turbulence, material properties, boundary condition and initial condition would be done.

4.4.3.1 Basic Setting – Transient Analysis Type

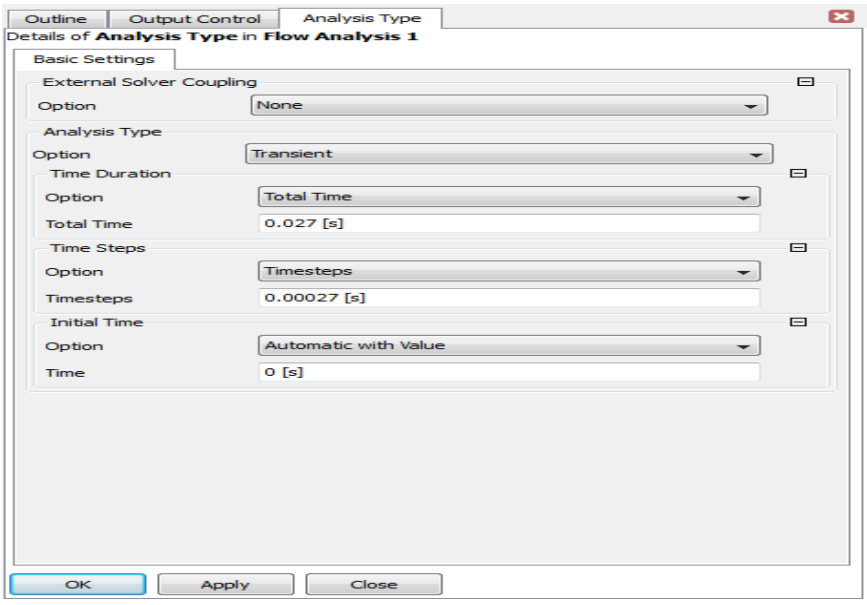

4.4.3.2 Boundary Details

Every domain must have boundary conditions applied to it and can be in various forms i.e inlets, outlets, walls. To solve the governing differential equations they have to be closed by specifying boundary conditions. This section contains a list of stationery boundaries.

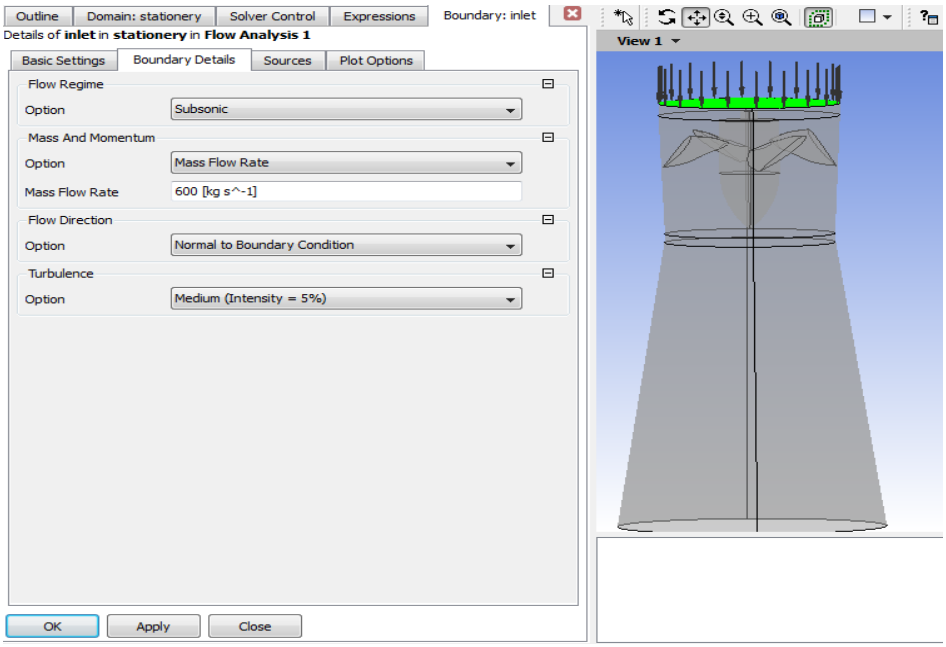

Figure 4.10: Inlet boundary details

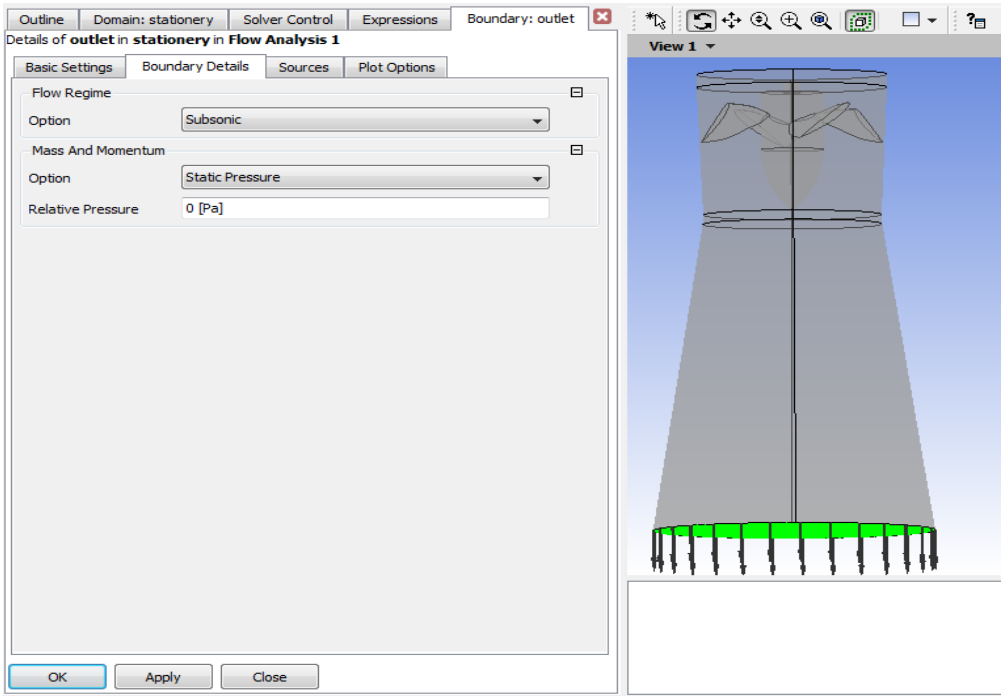

Figure 4.11: Outlet boundary details

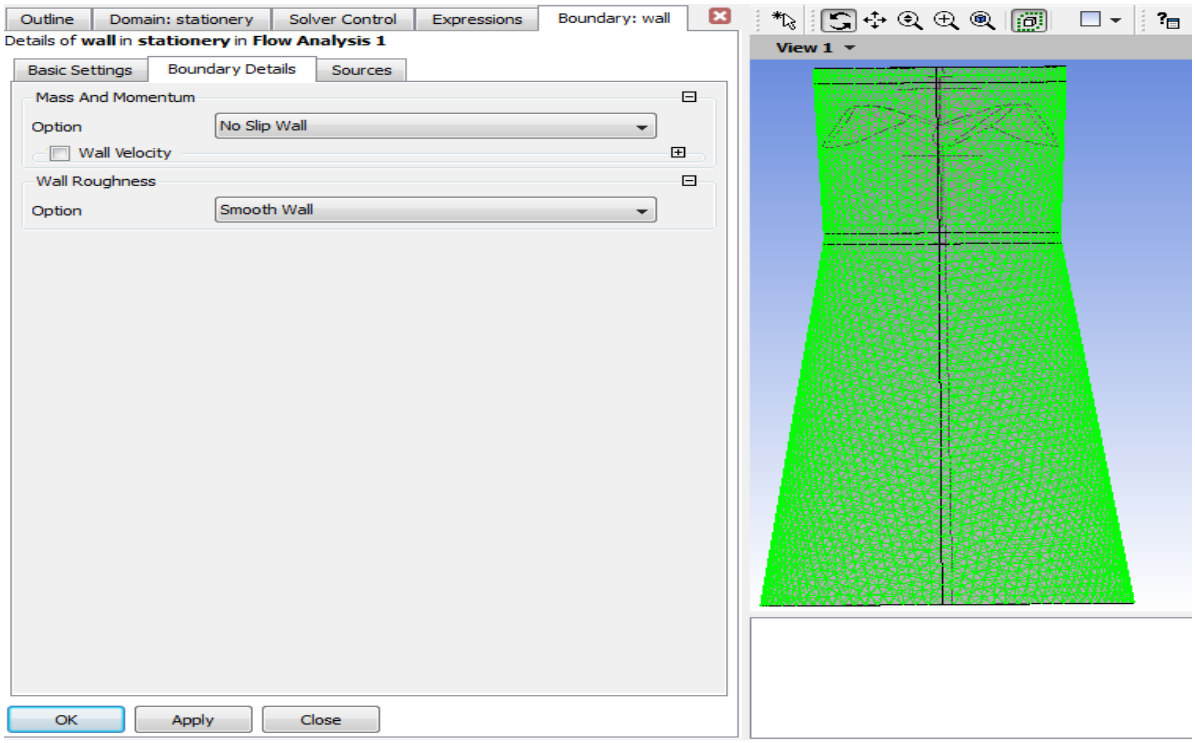

Figure 4.12: Boundary Wall details

4.4.3.3 Details of Flow Domain

4.4.3.3.1 Rotating Fluid Domain

In order to set up the rotating frame of reference, the runner was set up as a rotating domain.

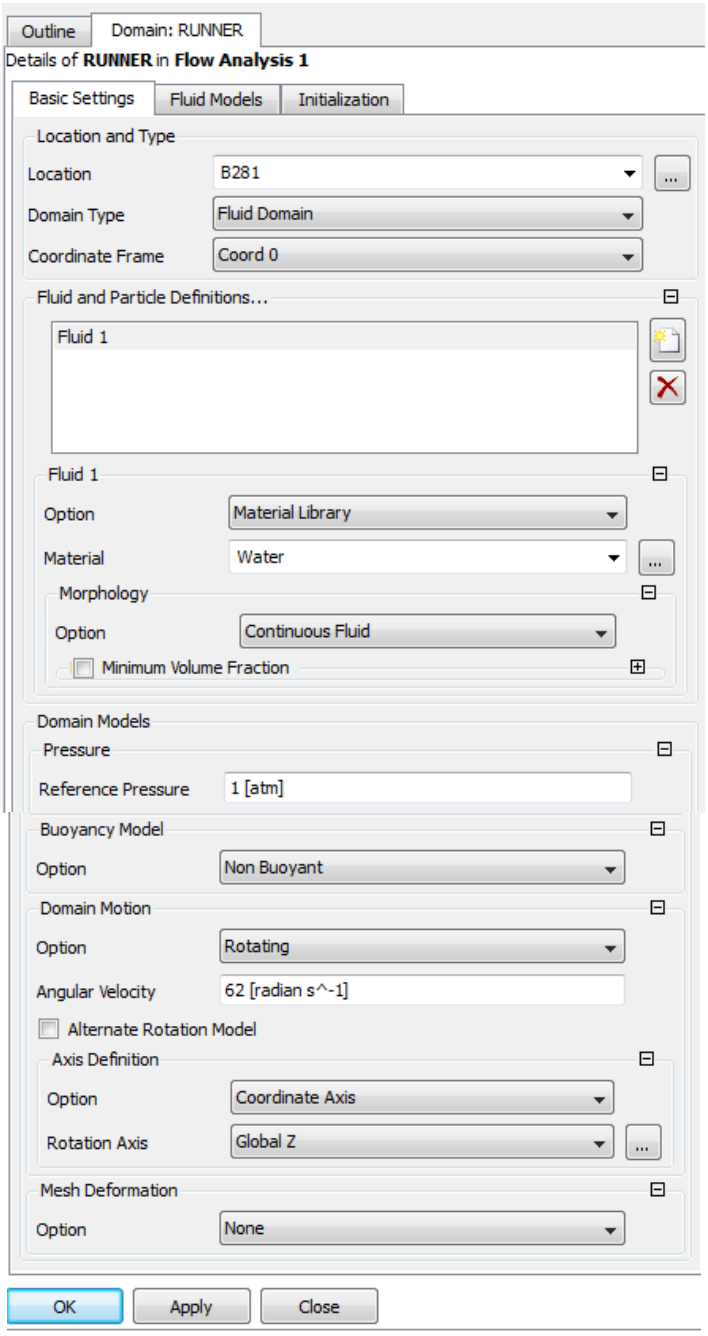

Figure 4.13: Domain Type, material selection, reference pressure and axis of rotation

4.4.3.3.2 Details of Stationary Fluid Domain

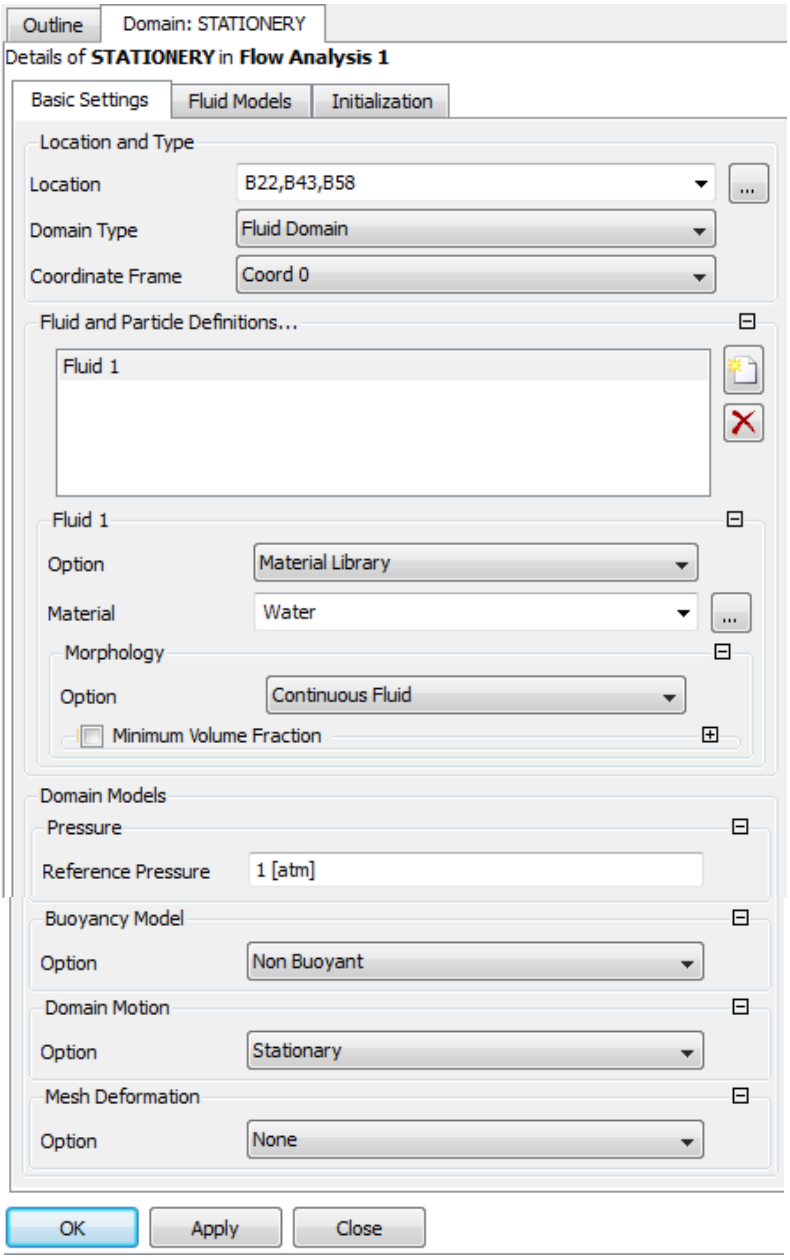

Figure 4.14: Domain model, material selection, reference pressure setting

4.4.3.4 Interface between Rotating and Stationary Domain – Top interface

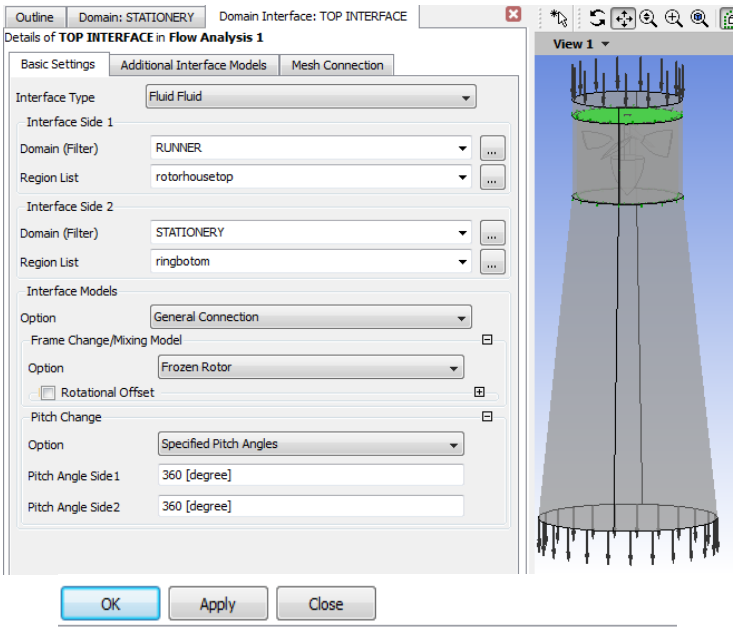

Figure 4.15: Top domain interface b/n the rotating and stationary domain

4.4.3.5 Interface between Rotating and Stationary Domain – Outer interface

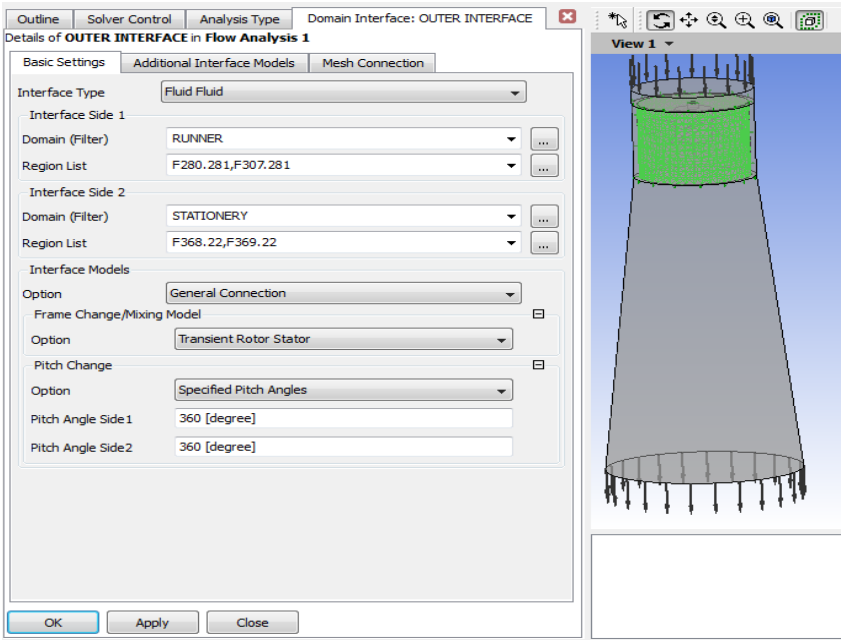

Figure 4.16: Outer interface b/n rotating and stationary domain

4.4.3.6 Interface between Rotating and Stationary Domain – Bottom interface

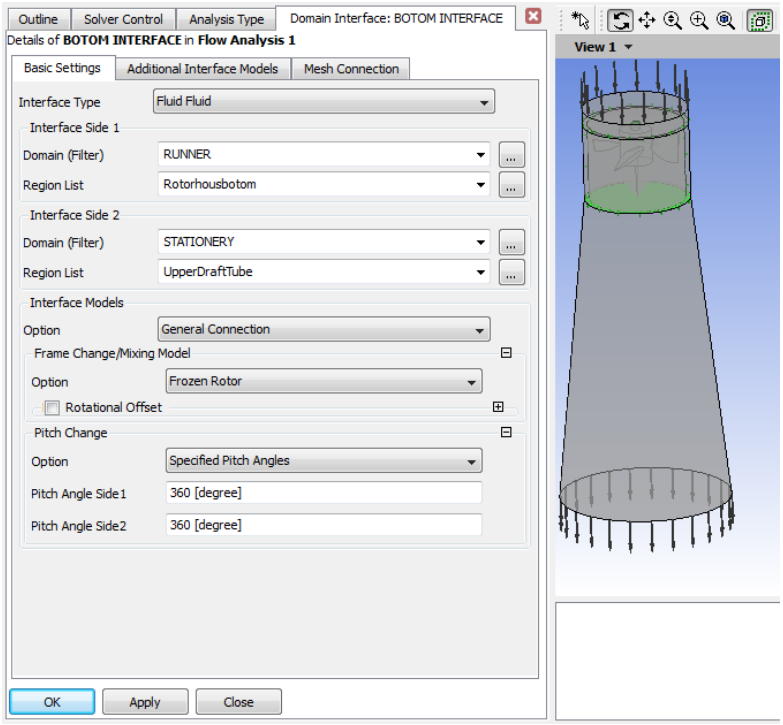

Figure 4.17: Bottom interface b/n rotating and stationary domain

4.4.3.7 Solver Control

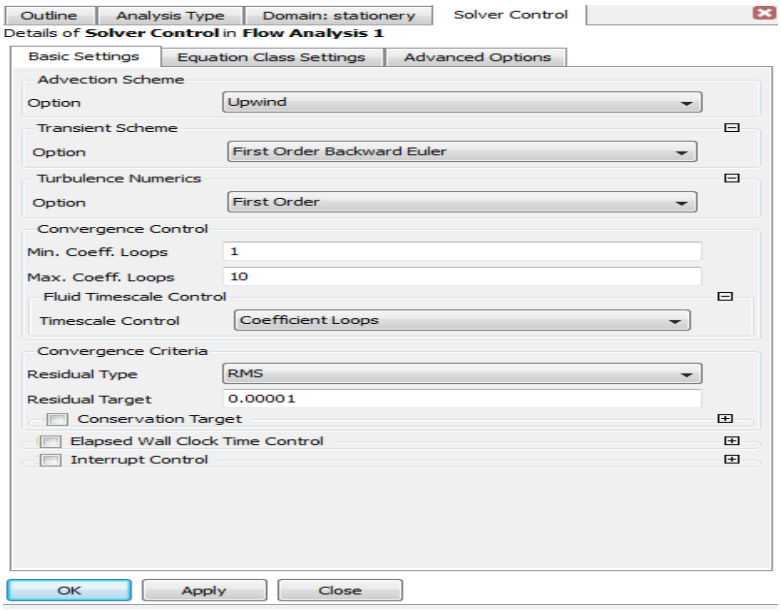

Figure 4.18: Basic setting for the solver

4.4.3.8 Output Control

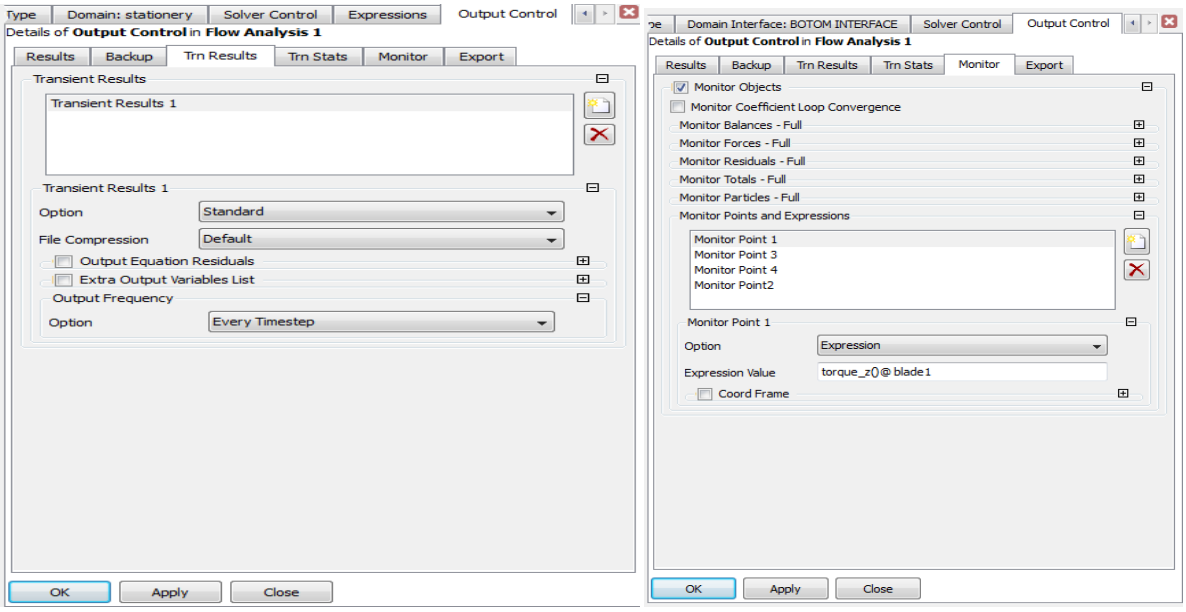

Figure 4.19: Basic setting for the Out Put Control

4.4.3.8 Expression

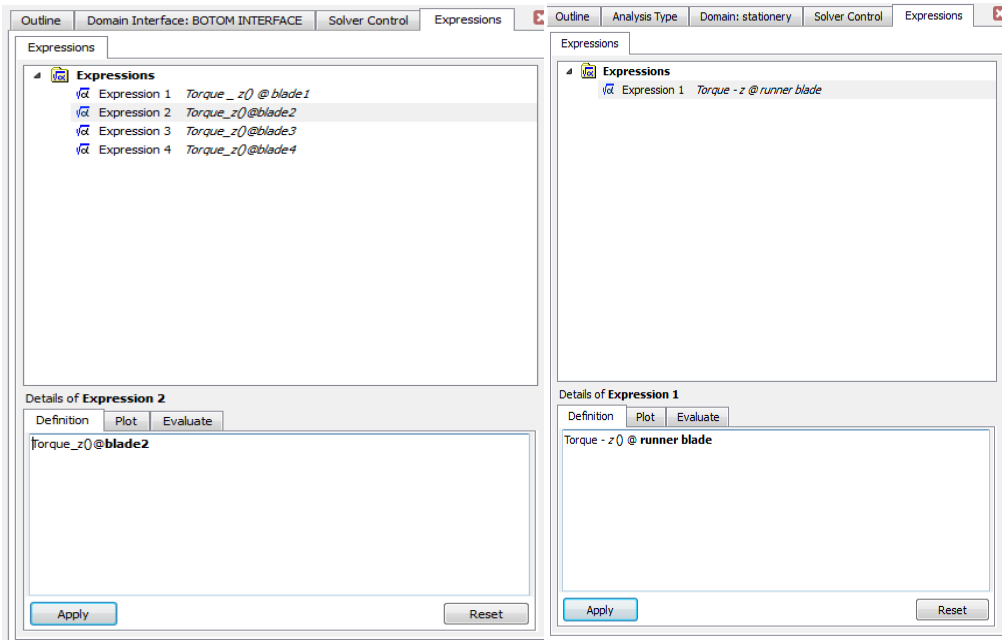

Figure 4.20: simple expressions for torque in the surface of each blade

4.4.3.9 Qualitative results for Transient

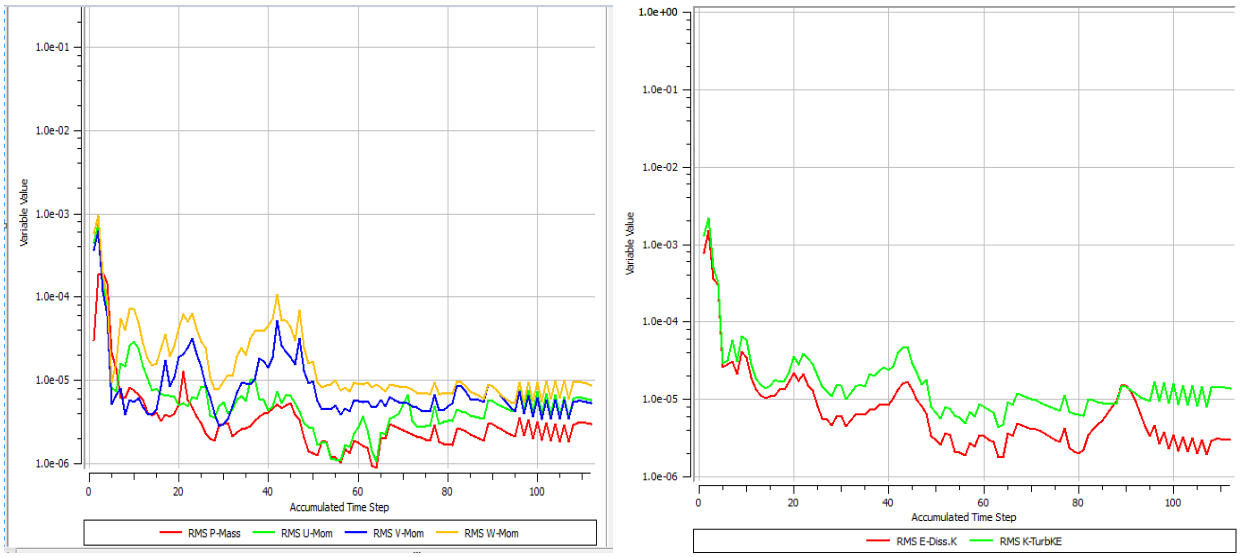

Figure 4.21: Iteration residual for momentum and mass (left) for eddy dissipation and turbulent kinetic energy (right)

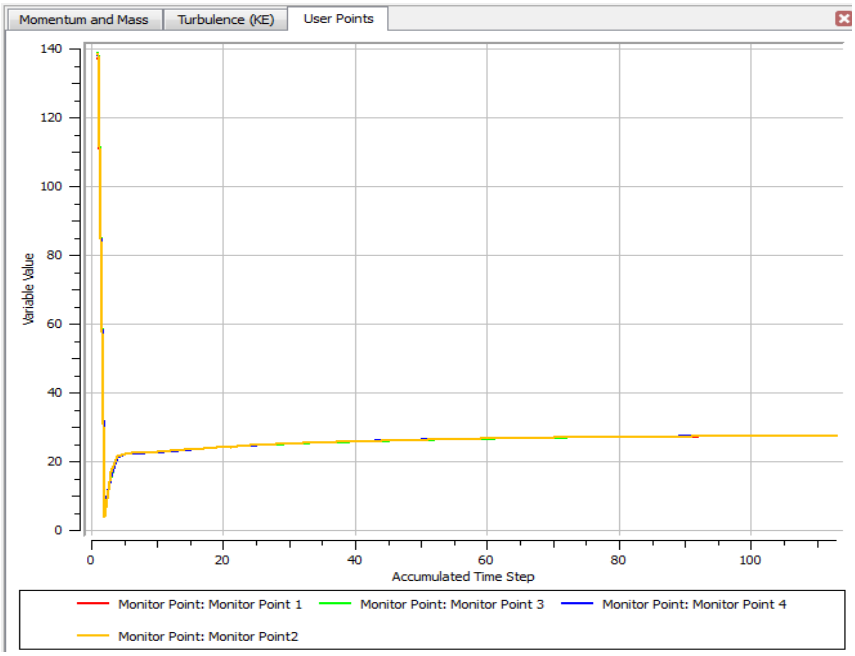

Figure 4.22: Torque on each blade surface is monitored

CHAPTER FIVE

RESULTS AND DISCUSSION

5.1 Introduction

In this chapter, results of the designed and CFD analysis of a micro Kaplan turbine runner are presented. The concept, formulas, graphs and tables discussed in previous chapters are used as input for this chapter to evaluate the performance of runner. In the CFD simulation, the flow has been simulated for a value of rotational speed and fluid flow rate varying from 375 rpm to1500rpm and 0.1m3/s to 1.0 m3/s respectively. Analyzing and discussing the computed results of all design variables in detail to identify the optimum performance of runner are presented in this chapter. Effect of fluid flow rate, runner speed and blade inclination angle to hub on the runner performance are shown on the characteristic curve. Runner optimization is also discussed in detail. Based on the computed CFD results disused below, comparison of efficiency of the runner with other similar work which was done by other researcher published internationally is carried out.

5.2 Flow pattern Inside the Runner

5.2.1 Flow Pattern of Velocity Streamline

Fig.5.1 Indicates variations of velocity streamline patterns in runner from inlet to outlet. It is observed that there is a change in velocity inside runner; it increases from its inlet to outlet as pressure energy of water is converted due to turbine runner rotation.

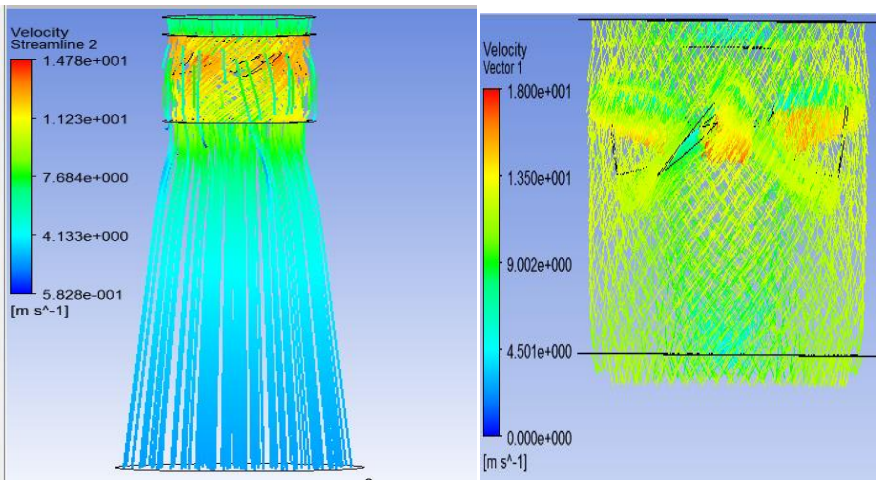

Figure 5.1: velocity stream line flow of turbine runner (left) Velocity vector (right)

5.2.2 Contours of Velocity

The contour diagrams in this section shows the velocity contours in stationery frame.

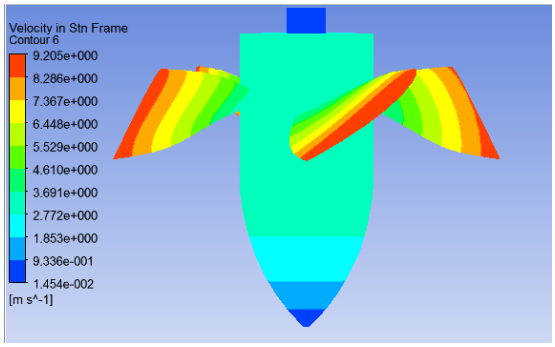

Figure 5.2: Contours of velocity in stationery frame

The diagram in Fig.5.2 describes the velocity contour diagram result obtained from ANSYS CFX. The velocity in the contour increases with the color goes from deep blue to red.

5.2.3 Pressure Contours Analysis

The pressure difference between pressure and suction surface of runner blade firstly increases from leading edge as water strikes on the blade and then decreases smoothly to meet towards the trailing edge. Pressure contours at constant flow rate of 0.6m3/s and rotational speed 600 (design condition) rpm are shown in Fig. 5.3

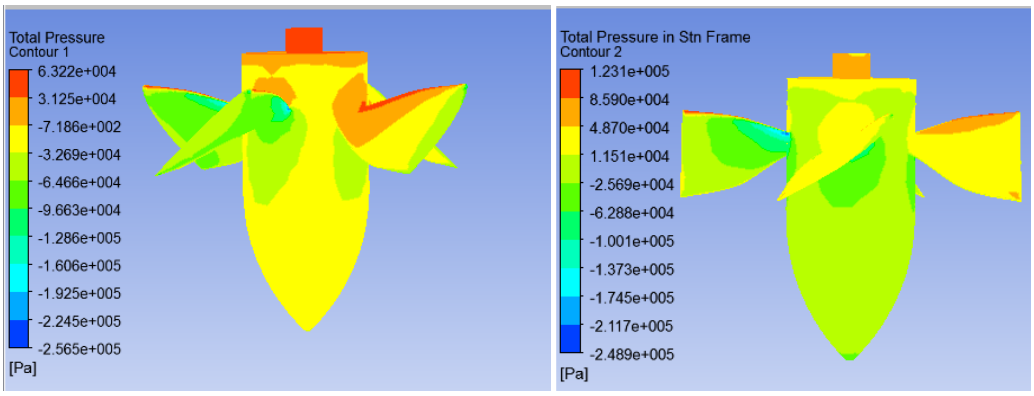

Figure 5.3: pressure contour runner surface of total (left) in stationery frame (right)

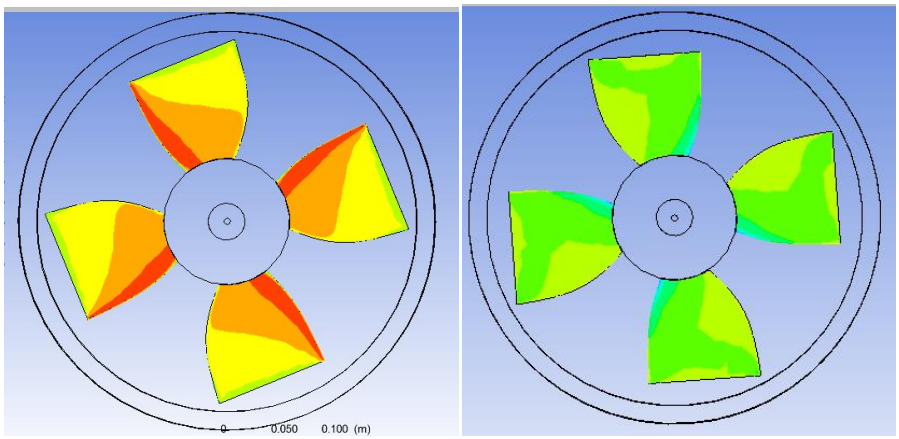

Figure 5.4: pressure contours on blade surface: pressure side (left) suction side (right)

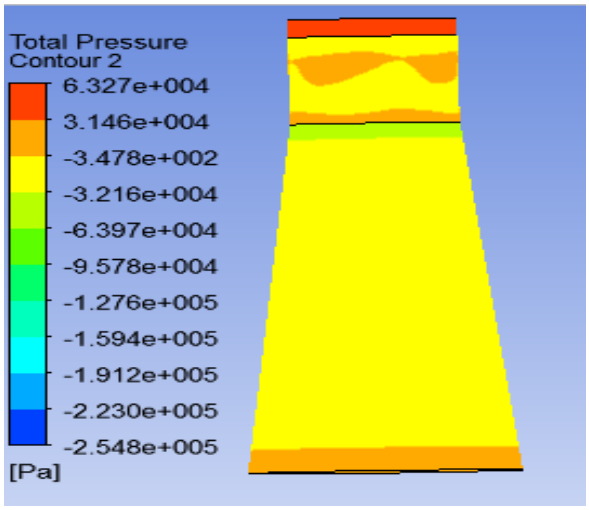

Figure 55: Total pressure on a mid-axial section of the whole domain

5.3 CFD Based Runner Performance Analysis

The following section contains the results from the CFD simulation of Kaplan turbine runner. The simulation was performed based on the provided quantities of input data's discussed in the previous sections; it was performed repeatedly by varying parameters that have a controlling effect over the output to find optimum solutions. It was carried in ANSYS-CFX by importing the 3D model file saved in Solid-Work as (.stp).The simulation of CFD software provides the results of optimized runner and its analysis. The output of the simulation is a list of parameters like torque (T), power output (P) and efficiency (η). It was done by varying/changing load of the turbine i.e. keeping first the flow regulator (δ) at constant position but varying rotational speed (n) of the runner and again keeping the speed (n) constant but varying fluid flow rate (Q).

The variations of hydraulic efficiency and power output with speed and flow rate are shown in on the characteristic curve Fig.5.5 and Fig.5.7 respectively. Hydraulic efficiency and power output show a parabolic variation with speed which is a characteristic of an axial flow turbine. The runner is found to have a maximum hydraulic efficiency of 91.6% at the value of design point i.e at a discharge and rotational speed of 0.6m3/s and 600 rpm respectively. Fig. 5.6 shows variations of torque developed on runner blade with flow rate keeps constant but varying runner speed. It is seen from the graphs that total torque decreases with increasing runner speed.

5.3.1 Simulation Result at Different Rotational Speed at Flow Rate Constant

Flow rate was kept constant while runner speed varied. CFD software simulates the designed model of runner using the specified input boundary conditions displayed in a Table 5.1. The software performs a number of simulations to evaluate the performance. Fig 5.5 shows both power and efficiency decreases with increasing runner speed because of higher pressure loss at high rotational speed in turbine runner as pressure energy is converted to kinetic energy. With the given values of constant and variable input parameters, equations of mass and momentum are solved numerically on discretized volume and torque on a blade is provided as output by the solver. The power output was calculated using the torque developed on the runner blades and rotational speed Eqn. (5.1). The total torque acting on a runner is the resultant of pressure and viscous moments. The hydraulic efficiency was obtained by dividing output to input power.

$P = T \omega$ (5.1)

Where:

P = power developed by the turbine in (watts)

T= Torque developed on the runner blade (N-m)

ω = angular speed (radian/s)

Table 5.1: The input and CFD simulated results of runner by varying the speed with the flow rate kept constant

S_n	At flow rate (Q = 0.2m3/s)					
S_1	Runner Speed (rpm)	350	500	600	1000	1500
	Torque (Nm)	228.04	188.18	151.6	40.6	1.25
	Output power (Kw)	8.38	11.17	10.87	7.644	0.2
	Efficiency (%)	59	76	74	52	1.3
S_2	At flow rate (Q = 0.4m3/s)					
	Runner Speed (rpm)	350	500	600	1000	1500
	Torque (Nm)	269.12	238.5	201.6	90.21	1.28
	Output power (Kw)	9.89	12.52	12.7	9.27	0.2
	Efficiency (%)	67.28	85.17	86.4	64.4	1.3
S_3	At flow rate (Q = 0.6m3/s)					
	Runner Speed (rpm)	350	500	600	1000	1500
	Torque (Nm)	280.11	247	209.6	98.5	1.3
	Output power (Kw)	11	13.04	13.5	10.29	0.2
	Efficiency (%)	74.83	89.4	91.6	71	1.4
S_4	At flow rate (Q = 0.8m3/s)					
	Runner Speed (rpm)	350	500	600	1000	1500

	Torque (Nm)	2799.2	248.06	209.2	98.2	1.27
	Output power (Kw)	10.26	13.02	13.18	10.3	0.2
	Efficiency (%)	69.8	88.57	89.66	70	1.3
S_5	At flow rate (Q = 1.0m3/s)					
	Runner Speed (rpm)	350	500	600	1000	1500
	Torque (Nm)	278.13	246.26	208.4	97.2	0.0013
	Output power (Kw)	10.22	12.93	13.13	10.23	0.2
	Efficiency (%)	69.5	87.96	89.3	69.6	1.3

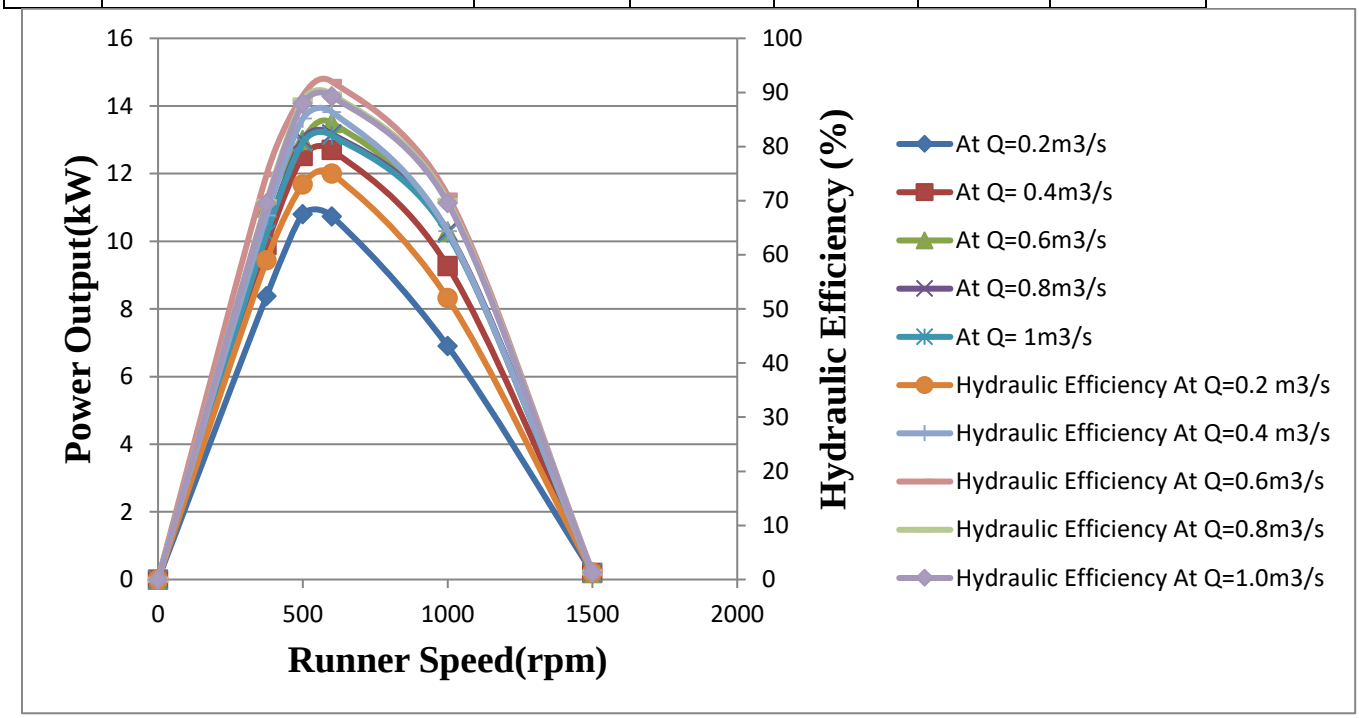

Figure 5.6: Dependence of efficiency and power output on runner speed with flow rate kept constant

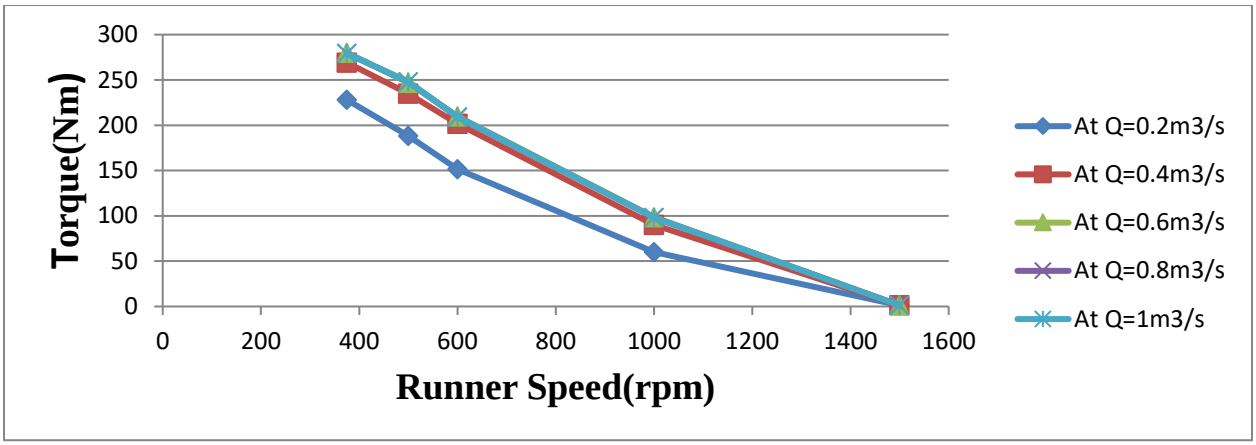

Figure 5.7: Dependence of torque on runner speed with flow rate kept constant

5.3.2 Simulation Results at Different Flow rate keeping Speed Constant

For constant dimensions turbine runner performance were evaluated at different flow rate while keeping all speed of the runner is constant. Efficiency of runner increases rapidly until it reaches 91.6% which is at flow rate of 0.6m3/s and then increases slowly till it finally becomes almost constant as shown in Fig 5.7. This is due to change in total pressure loss from inlet to outlet in turbine runner is almost constant as the flow rate increases. The result is tabulated in Table 5.2

Table 5.2 The input and simulated CFD results by varying flow rate, keeping the speed constant

S_n	**Parameters**					
S_1	Runner Speed (N= 350rpm)					
	At flow rate (Qm3/s)	0.2	0.4	0.6	0.8	1.0
	Output power (Kw)	7.8	9.89	10.73	10.5	10.22
	Efficiency (%)	53	71	73.8	71.3	69.5
S_2	Runner Speed (N= 500rpm)					
	At flow rate (Qm3/s)	0.2	0.4	0.6	0.8	1.0
	Output power (Kw)	10.5	12.52	12.8	13.02	12.93
	Efficiency (%)	73	85.17	87.17	88.57	87.96

S_3	Runner Speed (N= 600rpm)					
	At flow rate (Qm3/s)	0.2	0.4	0.6	0.8	1.0
	Output power (Kw)	9.54	12.7	13.47	13.18	13.13
	Efficiency (%)	65	86.4	91.6	90	89.13
S_4	Runner Speed (N=1000rpm)					
	At flow rate (Qm3/s)	0.2	0.4	0.6	0.8	1.0
	Output power (Kw)	4.3	9.47	10.29	10.3	10.10
	Efficiency (%)	35	64.4	70	70	69.6
S_5	Runner Speed (N= 1500rpm)					
	At flow rate (Qm3/s)	0.2	0.4	0.6	0.8	1.0
	Output power (Kw)	0.196	0.201	0.205	0.20	0.198
	Efficiency (%)	1.3	1.3	1.3	1.3	1.3

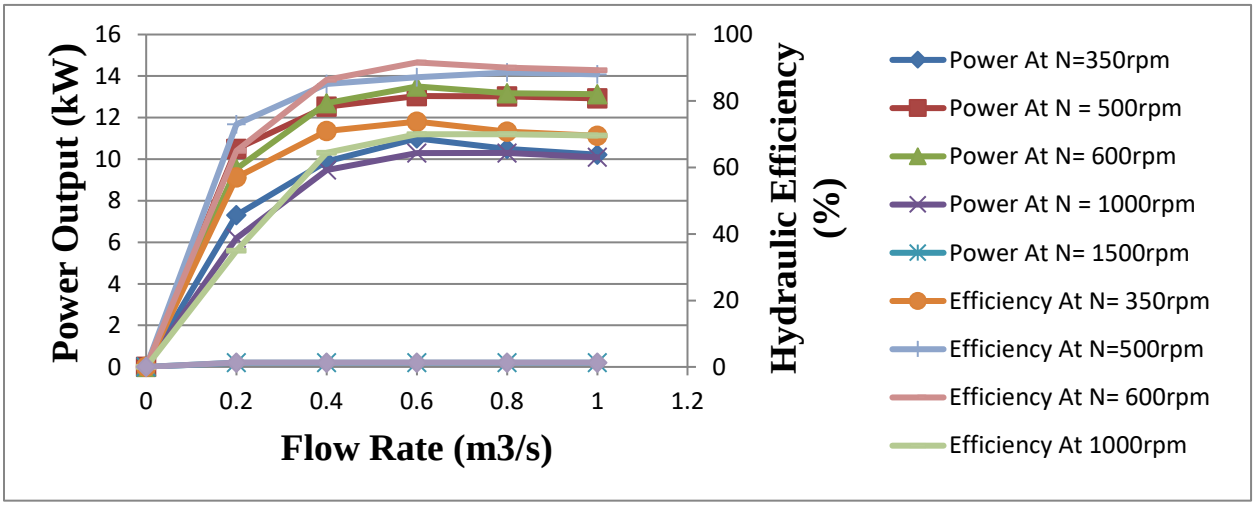

Figure 5.8: Variation of efficiency and power by varying fluid flow rate with speed constant

5.4 Optimization of the Runner

The designed runner was optimized with CFD by adjusting the blades inclination angle to hub to achieve a higher tangential velocity difference (ΔC_u) of the inlet and outlet edges of the runner (C_{u1} and C_{u2}) which would help to achieve a better efficiency.

Here, by following a similar methods to A. Bashir J. et. al [10] optimization of the runner was performed by changing the blade inclination angle (θ = 48°, 52°, 56°) to hub side. CFD loads (mass flow rate and runner speed) were used as input boundary conditions to perform the CFD analysis and were varied/changed in the simulation to investigate its impact on the total torque, power and efficiency and the results are given in the following tables and graphs below.

Table 5.3 Results of the optimized runner at constant flow rate

S.No	Q (m3/s)	N (rpm)	Options								
			At θ = 48°			At θ = 52°			At θ = 56°		
			T(N-m)	P(Kw)	η(%)	T(N-m)	P(Kw)	η(%)	T(N-m)	P(Kw)	η(%)
1	0.6	0	0	0	0	0	0	0	0	0	0
2		375	243.19	9.55	65	280.11	11	74.83	252.61	9.92	67.48
3		428	234.27	10.5	72.43	268.6	12.05	81.97	243.19	10.9	74.15
4		500	221.23	11.61	79	249.06	13.03	88.7	229.18	12	81.63
5		600	197.35	12.4	84.35	214.4	13.47	91.6	204.35	12.84	87.35
6		750	156.61	12.3	83.67	166.54	13.15	90	161.7	12.7	86.3
7		1000	100.27	10.4	71.43	98.5	10.29	70	101.22	10.6	72
8		1500	3.76	0.59	4	1.3	0.206	1.4	5.6	0.88	6

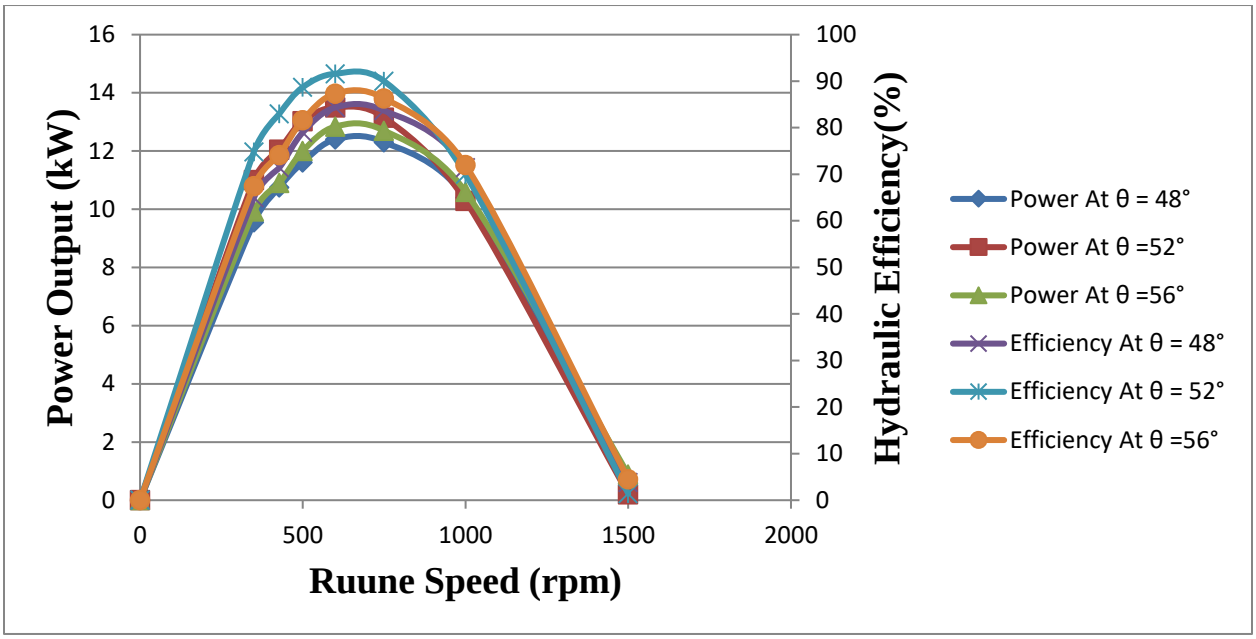

Figure 5.9: Graph of power and efficiency with different runner speed at flow rate constant

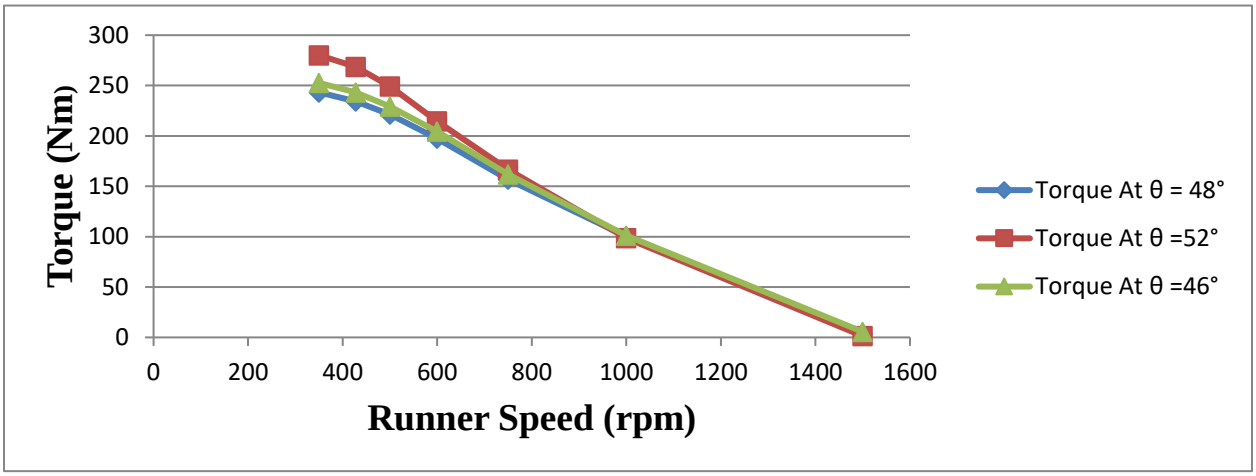

Figure 5.10: Graph of Torque vs Runner Speed at constant flow rate (Q = 0.6m3/s)

Table 5.4 Results of the optimization by varying flow rate at constant runner speed (N=600rpm)

No	Q(m3/s)	N(rpm)	Options					
			At θ = 48°		At θ = 52°		At θ = 56°	
			P(Kw)	η(%)	P(Kw)	η(%)	P(Kw)	η(%)
1	0.1	600	0.6	4	0.88	6	0.73	5
2	0.2		9.11	62	9.5	65	9.33	63.5
3	0.3		11.54	78.5	11.4	81	11.4	80
4	0.4		12.2	83	12.4	86.5	12.3	85.5
5	0.5		12.49	85	13	89	12.76	87.5
6	0.6		12.79	87	13.47	91.6	13	89
7	0.7		12.76	86.8	13.2	90	13.01	88.6
8	0.8		12.71	86.5	13.18	89.7	12.89	88.4
9	0.9		12.67	86.2	13.15	89.5	12.85	88.1
10	1.0		12.64	86	13.13	89.3	12.83	88

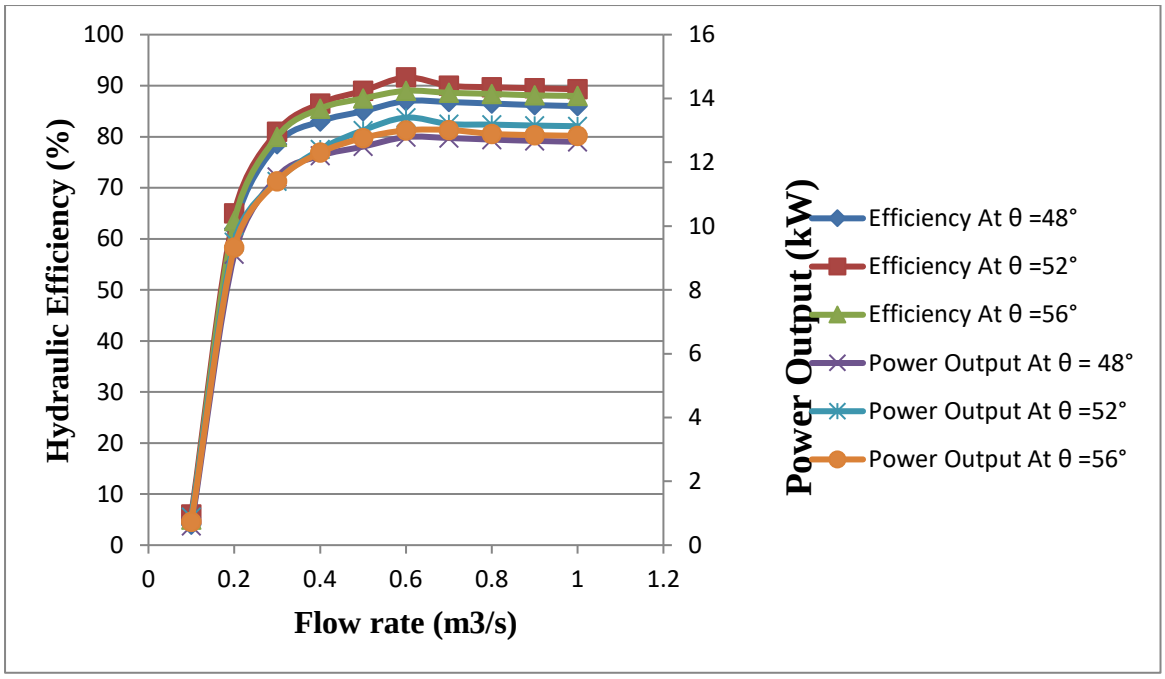

Figure 5.11: Graph of Power output and efficiency with different fluid flow rate at constant runner speed (N=600rpm)

5.5 Verification of Simulation Results

After CFD analysis it becomes very important to verify the results achieved. Verification is required for the assessment of the accuracy of computational model. This is achieved by comparing CFD results of the present work with that of V. chamber, R. Khare research work [8] published internationally with the goal being a verification of CFD model. The analysis has been carried out on the designed runner geometry by varying the loads.

The current verification of this model should be restricted to efficiency measurements and nothing else. Thus, the verification in this thesis only concerns to the efficiency of runner and is tabulated in Table 5.7. The specification of the turbine includes numerical simulation which has been carried out for an axial flow. Geometric dimensions and details of boundary condition are elaborated in Tables (5.5) and (5.6) respectively.

Table 5.5: Geometric dimensions of V.Chandrakar, R. Khare turbine model [8]

Type of turbine	Vertical axial flow Kaplan turbine
Type of casing	Spiral type
Type of draft tube	Elbow type
Diameter of turbine runner	0.400 m
Number of guide vanes	28
Number of stay ring	12

Table 5.6: Details of boundary conditions of V.Chandrakar, R. Khare [8] work

Boundary wall	Smooth with no slip
Input boundary condition	mass flow rate specified as
	0.525 m^3/s for 35^o G.V.O
	0.620 m^3/s for 40^o G.V.O
	0.714 m^3/s for 50^o G.V.O
Outlet boundary condition	Pressure at draft tube outlet as 0 atm.
Stationary blade rows	stay ring and guide vanes
Rotating blade row	Runner
Type of interfaces	Fluid-Fluid
Interface model	General connection

Table 5.7: Characteristic future of the designed 3D model of present and Dr. R. Khare work [8]

Items	**Dr. R. Khare work[8]**	**Present work**
Type of turbine	Vertical axial Kaplan turbine	Vertical axial Kaplan turbine
Type of draft tube	Elbow type	Cone type
Tip diameter	40cm	40cm
Boundary wall	Smooth with no slip	Smooth with no slip
Input boundary condition	mass flow rate	mass flow rate
Outlet boundary condition	Pressure at outlet 0 atm.	Pressure at outlet 0 atm.
Type of interfaces	Fluid-Fluid	Fluid-Fluid
Interface model	General connection	General connection
Loading condition	Guide Vane Opening	Blade inclination angle

Table 5.8: Comparison of CFD results of the present and Dr. Ruci Khare work[8]

Dr. Ruci. Khare work[8]				**Present work**		
Boundary conditions				Boundary conditions		
Input Q (m3/s)	Output P(atm)	CFD results (%)	Experimental results (%)	Input Q (m3/s)	Output P (atm)	CFD results (%)
0.52	0	91.5	89.2	0.5	0	89
0.62	0	92	90.3	0.6	0	90
0.714	0	90.8	88.5	0.7	9	89.6

From the results displayed above (Table 5.8) observed that, the hydraulic efficiencies obtained using the CFD simulation of designed runner model of both the present and published work are close enough to be verified. The slight difference was created due to the change of impute boundary condition of fluid flow rate.

CHAPTER SIX

CONCLUSION AND RECOMMENDATION

This chapter summaries the outcomes of the research and reflects on the goals set for the success to meeting them. Summary of the developed work, contributions towards the improvement of the existing facilities and recommendations for the future work also are provided.

6.1 Conclusion

The aim of this study is to design, model and CFD analysis of a micro Kaplan turbine runner. To accomplish the aim of the study, the geometry of Kaplan turbine runner was selected based on the flow rate and gross head of water available in Denkaka village. Deterring the basic dimensions/size of runner, 3-D modeling and computational fluid dynamic analysis were performed for the selected turbine runner profile. The verification of the present work with the previous researcher was also done. The important findings and their consequences are as follows.

- The average flow rate of the water is 0.6m^3/s and it was considered as the lowest flow rate that exists in the river since it was measured during late summer.
- The turbine runner profile was designed for the constant hub and outer diameter while varying the partial radius to find the cord length and angle of twist. Finally the 3-D modeling of the runner and draft tube were made based on the above data and the assembled of this profile was used for the input of CFD analysis.
- A tetrahedral mesh type with 1.4 million element size and 0.27 million nodes for rotating domain and hexahedral mesh type with 0.021 million element size and 0.0048 million nodes for stationary domain were chosen to descretize the profile.
- The velocity contour and pressure contour were developed and identified the position where maximum and minimum values occur.
- The simulation was performed by varying runner speed from 0 to 1500 rpm, while keeping the flow rate constant. The maximum power output of 13.47 kW was obtained at the designed value of 600 rpm, 0.6 m^3/s and corresponding torque of 209.61 Nm

with maximum hydraulic efficiency of 91.65%. Whereas while varying the flow rate from 0.1 to 1 m^3/s while keeping the speed constant, the maximum power output was obtained at 0.6 m^3/s.

- The optimization of the runner profile were done and found that the suitable blade inclination angle to hub side of 52° for varying speed and flow rate cases considered.
- Comparison of the present CFD results with the other researcher was carried out. The maximum efficiency regime specified by both works was nearly same and are reasonably acceptable.
- Prediction of turbine performance by CFD gives the idea to know the flow behavior inside the turbine model and get the information about the intricacy of flow pattern.

This present work can be used for the input while designing and implementing the electricity generation project in the specified site.

6.2. Contributions of the Developed Work

The design methodology, coupled with 3D model of turbine runner tools and CFD analysis, enables to achieve efficient turbine runner design.

The thesis work covers the development of the Solid-Work codes to accelerate the iterative design process involving extensive CFD applications. Once the CFD result verification is accepted, the designed 3D model of runner was ready to provide great contribution on installing of complete hydro turbine to generate electricity. Achievement of runner design know-how is expected to create a positive impact on the development of hydropower industry in the country scale. From this we can conclude that as the manufacturing is performed in Ethiopia, this study will also have a great contribution on the procurement of qualified workers in the runner manufacturing area and attract new investments in the hydropower industry.

6.3 Recommendations

The followings are some of the recommendations and future works used for further research and developments related to the present work.

The selected site should have better potential suitable for storage based and run of river type hydro power developments across the River. Accessing of this may be difficult so a concerned body should be carried out a detailed study allocating more time and finance.

Future work: The procedure described in the thesis can be extended for transient investigations using CFD tools which require larger computing capacity. Unsteady simulations covering the rotor-stator interactions, draft tube vortices can be investigated in order to improve the turbine design. Future works may also consist of the application of the design methodology to other types of turbines.

The major areas for further search should be.

- Accurate measurement of the design data such as, flow rate at the selected site.
- Detailed design of each component.

APPENDICES

Table 7.1: Vapor pressure of water

t/℃	0	2	4	6	8	10	12	14	16	18
0	0.6121	0.706	0.8135	0.9353	1.0729	1.2281	1.4027	1.5989	1.8187	2.0646
20	2.3392	2.6452	2.9857	3.3638	3.7809	4.2452	4.7582	5.324	5.9472	6.6324
40	7.3848	8.2096	9.1126	10.1	11.117	12.352	13.632	16.023	16.534	18.173
60	1.948	21.869	23.946	26.188	28.605	31.21	34.013	37.01	40.24	43.704
80	47.416	51.388	55.636	60.174	65.018	70.183	75.685	81.542	87.771	94.39
100	101.42	108.87	116.78	125.15	134.01	143.38	153.25	163.74	174.77	186.41

Table 7.2: Coordinate points for leading side

Leading side – upper edge		
X-axis (mm)	Y-axis (mm)	Z-axis (mm)
0.01502	0.02212	0.00
0.01191	0.01968	0.00
0.00915	0.01724	0.00
0.00675	0.01478	0.00
0.0047	0.01232	0.00
0.00302	0.00986	0.00
0.0017	0.00739	0.00

Leading side – lower edge		
X-axis (mm)	Y-axis (mm)	Z-axis (mm)
0.01502	-0.01917	0.00
0.01191	-0.01734	0.00
0.00915	-0.01543	0.00
0.00675	-0.01344	0.00
0.0047	-0.01139	0.00
0.00302	-0.00926	0.00
0.0017	-0.00705	0.00

0.00076	0.00493	0.00	0.00076	-0.00478	0.00
0.00019	0.00246	0.00	0.00019	-0.00243	0.00
0.00	0.00	0.00	0.00	0.00	0.00

Table 7.3: Coordinate points for trailing side

Trailing side - upper edge			Trailing side - lower edge		
X-axis (mm)	Y-axis (mm)	Z-axis (mm)	X-axis (mm)	Y-axis (mm)	Z-axis (mm)
1.00	0.00	0.00	1.00	0.00	0.00
0.99748	0.00178	0.00	0.99748	-0.00145	0.00
0.99291	0.00272	0.00	0.99291	-0.00178	0.00
0.98705	0.00392	0.00	0.98705	-0.00221	0.00
0.98019	0.00531	0.00	0.98019	-0.00271	0.00
0.97248	0.00685	0.00	0.97248	-0.00326	0.00
0.96406	0.00852	0.00	0.96406	-0.00387	0.00
0.95499	0.01029	0.00	0.95499	-0.00452	0.00

Table 7.4: Coordinate points for hub side

Hub side – upper edge			Hub side – lower edge		
X-axis (mm)	Y-axis (mm)	z-axis (mm)	X-axis (mm)	Y-axis (mm)	z-axis (mm)
0.000739	0.00082208	0.00	0.000739	-0.000679	0.00
0.000624	0.00075488	0.00	0.000624	-0.0006336	0.00
0.000517	0.0006874	0.00	0.000517	-0.0005863	0.00
0.000421	0.00061936	0.00	0.000421	-0.0005368	0.00
0.000333	0.00055104	0.00	0.000333	-0.0004855	0.00
0.000256	0.00048272	0.00	0.000256	-0.000432	0.00
0.000189	0.00041384	0.00	0.000189	-0.0003763	0.00
0.000132	0.00034496	0.00	0.000132	-0.0003189	0.00
8.46E-05	0.00027608	0.00	8.46E-05	-0.0002593	0.00
4.76E-05	0.00020692	0.00	4.76E-05	-0.0001974	0.00
2.13E-05	0.00013804	0.00	2.13E-05	-0.0001338	0.00
5.32E-06	0.00006888	0.00	5.32E-06	-6.804E-05	0.00
0.00	0.00	0.00	0.00	0.00	0.00

Table 7.5: Coordinate points for shroud side

Shroud side - upper edge		
X-axis (mm)	Y-axis (mm)	z-axis (mm)
0.000824	0.00099752	0.00
0.000683	0.00090835	0.00
0.000556	0.00081844	0.00
0.000441	0.00072816	0.00
0.000339	0.00063788	0.00
0.00025	0.00054686	0.00
0.000174	0.00045584	0.00
0.000112	0.00036482	0.00
6.29E-05	0.00027343	0.00
2.81E-05	0.00018241	0.00
7.03E-06	0.00009102	0.00
0.00	0.00	0.00

Shroud side - lower edge		
X-axis (mm)	Y-axis (mm)	z-axis (mm)
0.000824	-0.0008373	0.00
0.000683	-0.0007748	0.00
0.000556	-0.0007093	0.00
0.000441	-0.0006416	0.00
0.000339	-0.0005709	0.00
0.00025	-0.0004973	0.00
0.000127	-0.0004214	0.00
0.000112	-0.0003426	0.00
6.29E-05	-0.0002609	0.00
2.81E-05	-0.0001769	0.00
7.03E-06	-8.991E-05	0.00
0.00	0.00	0.00

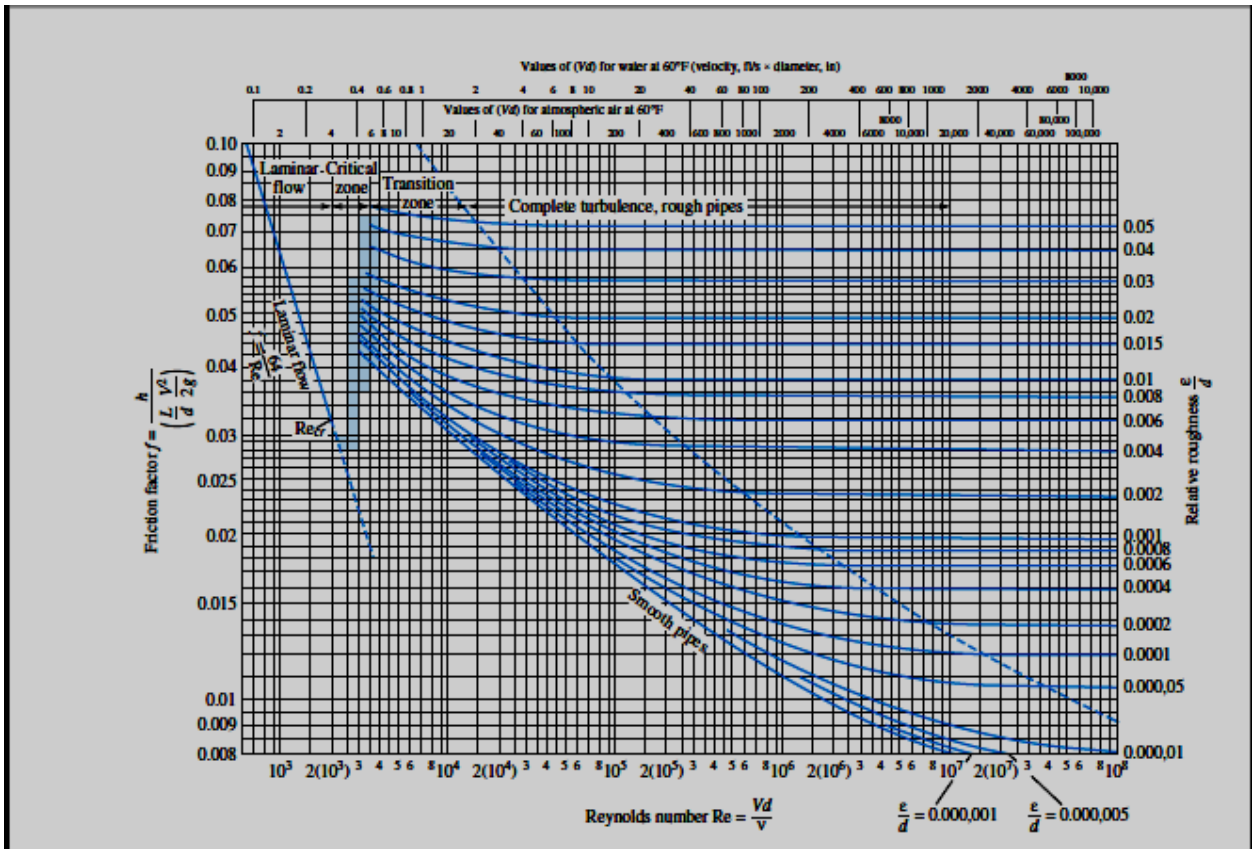

Figure 7.1: The Moody chart for pipe friction with smooth and rough walls [source: Frank M. White Professor of Mechanical engineering]

REFERENCES

[1]. http://cdn.intechopen.com/pdfs-wm/40550.pdf

[2]. Phommachanh, Junichi Kurukowa, Choi Nakijama, 2006, “Development of positive micro hydro turbine”.

[3]. Melessaw Shanko, TargetmMarket Analysis, Ethiopia’s Small Hydro Energy Market, December 2009.

[4]. Energy Efficiency and Renewable Energy, 2003, ‘’Wind & Hydropower Technologies Program Harnessing America’s abundant natural resources for clean power generation’’u.s department of energy

[5].Adiyanju, A.A., Technical Feasibility of Micro Hydro Installation Journal of Engineering and Applied Sciences 2009. 4(5,6): p. 324-334.

[6]. Singh, D., Micro Hydro Power Resource Assessment Handbook. 2009, APCTT: New Delhi,India.

[7]. Dominik Schmitz, 2006,’’ Developing a methodology for assessing the Sustainable Development impact of Small Scale CDM hydropower projects’’ Hamburg Institute of International Economic

[8].Vaibhav Chandrakar, Dr. Ruchi Khare Numerical Simulation for Unsteady Flow Analysis of Kaplan Turbine

[9].Timo Flaspohler (2007). Design of the runner of a Kaplan turbine for small hydroelectric power plants‖. Doctoral Thesis. Department of Environmental Engineering, Tampere University of Applied Sciences, Finland. Supervised by Jaakko Mattila.

[10]. L Motycak and J Obrovsky Analysis of the Kaplan turbine draft tube effect CKD Blansko Engineering, a.s., Capkova 2357/5, Blansko 67801, Czech Republic.

[11]. Y. Myint, H. Win Design and Flow Simulation of Runner Blade for Propeller Turbine Research Scholar, Dept of Mechanical Engineering, Mandalay Technological University. Mandalay, Myanmar,

[12]. Ruchi Khare (Dr.) "Design Optimization of Conical Draft Tube of Hydraulic Turbine", International Journal of Advances in Engineering, Science and Technology (IJAEST), ISSN: 2249-913x, Vol. 2 No. 1 Mar-May 2012.

[13]. Diaelhag Khalifa, Simulation of an axial flow turbine runner's blades using CFD Mechanical Engineering, King Abdul-Aziz University, Jeddah, KSA

[14]. Williams, A.A., and Simpson, R.G., "Application of computational fluid dynamics to the design of pico propeller turbines", Proceedings of the International Conference on Renewable Energy for Developing Countries - 2006

[15]. Yohannis Mitiku, A.Venkata et.al CFD simulation and optimization of very low head axial flow turbine runner, international journal of renewable energy development, 2015

[16]. Nabil H. Mostafa and Mohamed Adel Unsteady Numerical Simulation of Cavitation in Axial Turbine Mechanical Power Engineering Department, Engineering Faculty Zagazig University, Zagazig, 44519, EGYPT

[17]. Alie Wube Dametew. Design and Analysis of Small Hydro Power for Rural Electrification Global Journal of Researches in Engineering: F Electrical and Electronics Engineering.

[18]. U. Zope, Prof.Dr. P.S.Pingle. Micro hydropower turbines design. International Journal of Scientific & Engineering Research, Volume 5, December-2014

[19]. Adam2, P.S.a.I.K., Design, Simulation and Experimental of the Very Low Head Turbine with Minimum Pressure and Free Vortex Criterions. ijmme-ijens, 2011. 11 No: 01: p. 9-15

[20]. Guide on how to develop a Small Hydropower Plant. [21]. Aktan Temiz. Decision making on turbine types and capacities for run-of-river hydroelectric power plants a case study on eglence-1 hepp, 2013

[22]. Micro Hydro Power Resource Assessment Handbook Prepared for Asian and Pacific Centre for Transfer of Technology Of the United Nations – Economic and Social; Commission for Asia and the Pacific (ESCAP); By Dilip Singh; September 2009

[23]. Swe le minn, Htay Htay win, Myint Thein Design and Vibration Characteristic Analysis of 10kW Kaplan Turbine Runner Blade Profile May-2014, Vol.03, Issue.06

[24]. ABID. A.B. M. Analysis of propellers for micro hydro power for domestic and commercial loads Faculty of Mechanical Engineering University Malaysia Pahang, June 2013

[25]. M. Abubakar, S. Badshah, T. Ahmad, N. Rahman Modelling and Analysis of a very Low Head Kaplan Turbine Runner Blades for Rural Area of Punjab International Journal of Scientific & Engineering Research, Volume 5, Issue 7, July-2014 905 ISSN 2229-5518

[26]. A. CJ, design and implementation of a low cost grid-connected 10 kW hydro power system.

[27].http:www.kayelaby.npl.co.uk/chemistry/3_4/3_4_2.html Vapour pressure of water at temperatures between 0 and 360°C, Accessed 24 September 2007

[28]. Er. Shivam Saxena1, Mr. Rahul Kumar. Design of NACA 2412 and its Analysis International Journal of Engineering Research and General Science March-April, 2015

[29]. D.New, "Intro to Hydropower, Part 2: Measuring Head and Flow", Home Power 104/December 2004 & January 2005.

[30]. Gahlot, V.K., and Krishnamachar., "CFD approach for design optimization and validation for axial flow hydraulic turbine",

[31] .C. C. Warnick ,"Hydropower engineering'' University of Idaho Moscow